

# Analysis of Pipe Supports with a Trunnion Welded to the Main Piping Run

2013 TECHNICAL REPORT



# **Analysis of Pipe Supports with a Trunnion Welded to the Main Piping Run**

**3002001179**

Final Report, October 2013

EPRI Project Manager  
K. Coleman

## **DISCLAIMER OF WARRANTIES AND LIMITATION OF LIABILITIES**

THIS DOCUMENT WAS PREPARED BY THE ORGANIZATION(S) NAMED BELOW AS AN ACCOUNT OF WORK SPONSORED OR COSPONSORED BY THE ELECTRIC POWER RESEARCH INSTITUTE, INC. (EPRI). NEITHER EPRI, ANY MEMBER OF EPRI, ANY COSPONSOR, THE ORGANIZATION(S) BELOW, NOR ANY PERSON ACTING ON BEHALF OF ANY OF THEM:

(A) MAKES ANY WARRANTY OR REPRESENTATION WHATSOEVER, EXPRESS OR IMPLIED, (I) WITH RESPECT TO THE USE OF ANY INFORMATION, APPARATUS, METHOD, PROCESS, OR SIMILAR ITEM DISCLOSED IN THIS DOCUMENT, INCLUDING MERCHANTABILITY AND FITNESS FOR A PARTICULAR PURPOSE, OR (II) THAT SUCH USE DOES NOT INFRINGE ON OR INTERFERE WITH PRIVATELY OWNED RIGHTS, INCLUDING ANY PARTY'S INTELLECTUAL PROPERTY, OR (III) THAT THIS DOCUMENT IS SUITABLE TO ANY PARTICULAR USER'S CIRCUMSTANCE; OR

(B) ASSUMES RESPONSIBILITY FOR ANY DAMAGES OR OTHER LIABILITY WHATSOEVER (INCLUDING ANY CONSEQUENTIAL DAMAGES, EVEN IF EPRI OR ANY EPRI REPRESENTATIVE HAS BEEN ADVISED OF THE POSSIBILITY OF SUCH DAMAGES) RESULTING FROM YOUR SELECTION OR USE OF THIS DOCUMENT OR ANY INFORMATION, APPARATUS, METHOD, PROCESS, OR SIMILAR ITEM DISCLOSED IN THIS DOCUMENT.

REFERENCE HEREIN TO ANY SPECIFIC COMMERCIAL PRODUCT, PROCESS, OR SERVICE BY ITS TRADE NAME, TRADEMARK, MANUFACTURER, OR OTHERWISE, DOES NOT NECESSARILY CONSTITUTE OR IMPLY ITS ENDORSEMENT, RECOMMENDATION, OR FAVORING BY EPRI.

THE FOLLOWING ORGANIZATION, UNDER CONTRACT TO EPRI, PREPARED THIS REPORT:

**Structural Integrity Associates, Inc.**

## **NOTE**

For further information about EPRI, call the EPRI Customer Assistance Center at 800.313.3774 or e-mail [askepri@epri.com](mailto:askepri@epri.com).

Electric Power Research Institute, EPRI, and TOGETHER...SHAPING THE FUTURE OF ELECTRICITY are registered service marks of the Electric Power Research Institute, Inc.

Copyright © 2013 Electric Power Research Institute, Inc. All rights reserved.

# ACKNOWLEDGMENTS

---

The following organization, under contract to the Electric Power Research Institute (EPRI), prepared this report:

Structural Integrity Associates, Inc.  
11515 Vanstory Dr., Suite 125  
Huntersville, NC 28078

Principal Investigators

I. Perrin  
T. Sambor

This report describes research sponsored by EPRI.

---

This publication is a corporate document that should be cited in the literature in the following manner:

*Analysis of Pipe Supports with a Trunnion Welded to the Main Piping Run.* EPRI, Palo Alto, CA: 2013. 3002001179



# ABSTRACT

---

One configuration of pipe support that is gaining popularity, particularly on main steam and hot reheat high-energy piping, is the trunnion. In a trunnion support system, load is transferred from the main pipe to a hanger system through trunnions welded to the main pipe run. Welded trunnions are used in a variety of support configurations, and, in several cases, the support frame around the trunnion would have to be dismantled to permit inspection of the pipe-to-trunnion weld. In other configurations, only the insulation needs to be removed, but because this is not a pressure boundary weld, questions arise about the need to inspect the trunnion-to-pipe weld. An important consideration is that on modern high-energy piping systems fabricated from Grade 91 (or similar) steels, the trunnion-to-pipe weld will inevitably contain a creep-weak Type IV region within the heat-affected zone, which could be vulnerable to creep damage accumulation.

To provide some insight into the likelihood of creep or fatigue damage at the pipe-to-trunnion weld, a series of evaluations investigated sustained loads and temperature gradients (static and transient) that might affect the integrity of the weld. The objective of the report is not to provide detailed analysis of all trunnion configurations. Instead, this report highlights the most important parameters that affect the local stresses at the trunnion-to-pipe weld and establishes the typical stress magnitudes compared to other stresses in the piping system to help identify the relative importance of pipe-to-trunnion welds.

To identify which trunnions should be subject to more detailed analysis or inspection, various analyses were used to develop simple screening methods for static and transient thermal events. The report also provides guidance on the likely damage mechanisms and inspection techniques.

## **Keywords**

Creep  
Fatigue  
Grade 91  
High-energy piping  
Risk assessment  
Type IV





# CONTENTS

---

|   |            |
|---|------------|
| <b>1 INTRODUCTION .....</b>   | <b>1-1</b> |
| <b>2 STATIC LOADING.....</b>  | <b>2-1</b> |
| 2.1 Design Rules and Codes.....                                     | 2-1        |
| 2.2 Trunnions with In-Plane Loading .....                           | 2-5        |
| 2.3 Trunnions with Out-Of-Plane Loading .....                       | 2-10       |
| 2.4 Stress Distribution and Susceptibility to Type IV Cracking..... | 2-13       |
| 2.5 Conclusions from Static Loading Analysis .....                  | 2-16       |
| <b>3 STEADY STATE TEMPERATURES.....</b>                             | <b>3-1</b> |
| 3.1 Thermal Analysis Model .....                                    | 3-1        |
| 3.2 Results and Discussion for Steady State Thermal Analyses .....  | 3-4        |
| 3.3 Conclusions from Steady State Thermal Analyses .....            | 3-9        |
| <b>4 STEADY STATE TEMPERATURES.....</b>                             | <b>4-1</b> |
| 4.1 Transient Analysis Model .....                                  | 4-1        |
| 4.2 Results and Discussion for Transient Analyses .....             | 4-4        |
| 4.3 Conclusions from Transient Analyses .....                       | 4-9        |
| <b>5 SUMMARY AND RECOMMENDATIONS.....</b>                           | <b>5-1</b> |
| <b>6 REFERENCES .....</b>   | <b>6-1</b> |



# LIST OF FIGURES

---

|   |      |
|---|------|
| Figure 1-1 Schematics of trunnions and a riser clamp arrangement that utilize trunnions welded to the main pipe run.....  | 1-1  |
| Figure 2-1 General configuration of a pipe with a trunnion illustrating the directions of in-plane and out-of-plane loading .....   | 2-4  |
| Figure 2-2 Model of pipe and trunnion for analysis of static stresses (Case 3) .....  | 2-8  |
| Figure 2-3 Cut-away view showing a color contour plot of the axial stress distribution in the pipe and trunnion (Case 3) .....  | 2-9  |
| Figure 2-4 Distribution of stress in the pipe, and linearization to provide a stress to compare with ASME Code article and Timoshenko methods (Case 3) .....  | 2-10 |
| Figure 2-5 Cut-away view showing a color contour plot of the hoop stress distribution in the pipe and trunnion (Case 3) .....   | 2-12 |
| Figure 2-6 Distribution of hoop stress in the pipe, and linearization to provide a stress to compare with Timoshenko method (Case 3) .....  | 2-13 |
| Figure 2-7 Cut-away view of trunnion to pipe connection with annotation to indicate likely location of damage for different loading scenarios.....  | 2-15 |
| Figure 2-8 Photograph of a Type IV crack at the saddle of a nozzle connection in a Grade 91 piping system.....  | 2-15 |
| Figure 2-9 Color contour plot showing the spatial distribution of equivalent accumulated creep strain from a steady state creep analysis with no load applied to the trunnion (internal pressure only)..... | 2-16 |
| Figure 3-1 Typical finite element model for steady state thermal evaluation .....   | 3-4  |
| Figure 3-2 Color contour plot showing temperature (F) distribution for Case 1 with 1.7Btu/hr-ft <sup>2</sup> -F natural convection coefficient .....  | 3-6  |
| Figure 3-3 Color contour plot showing temperature (F) distribution for Case 1 with 0.2Btu/hr-ft <sup>2</sup> -F natural convection coefficient .....  | 3-6  |
| Figure 3-4 Color contour plot showing temperature difference (F) in Case 1 with 1.7Btu/hr-ft <sup>2</sup> -F natural convection coefficient .....   | 3-7  |
| Figure 3-5 Color contour plot showing temperature difference (F) in Case 1 with 0.2Btu/hr-ft <sup>2</sup> -F natural convection coefficient .....   | 3-7  |
| Figure 3-6 Fluid to weld temperature difference (F) as a function of insulation thickness for various heat transfer coefficients and configurations .....   | 3-8  |
| Figure 3-7 Fluid to weld temperature difference (F) as a function of trunnion length for various heat transfer coefficients, illustrating the effect of an end cap for the Case 1 configuration.....        | 3-9  |
| Figure 4-1 Typical finite element model for thermal transient evaluation .....  | 4-4  |

---

|  |     |
|--|-----|
| Figure 4-2 Color contour plot of the bending stress (ksi) at the base of the trunnion due to a heating transient in the pipe.....                          | 4-7 |
| Figure 4-3 Chart showing the through wall bending stress across the trunnion thickness and the linearization of the stress distribution (for Case 1) ..... | 4-8 |

# LIST OF TABLES

---

|   |      |
|---|------|
| Table 2-1 Sample of trunnion configurations from actual piping systems (all with in-plane loading) .....  | 2-6  |
| Table 2-2 Calculations of stress in trunnion and pipe for sample trunnion configurations using the stress calculations methods of Timoshenko and ASME article ..... | 2-7  |
| Table 2-3 Comparison of calculations for stress in the pipe created by the loading from the trunnion .....  | 2-7  |
| Table 2-4 Comparison of calculations for stress in the pipe created by the loading from the trunnion .....  | 2-11 |
| Table 3-1 Key geometric data for steady state heat transfer analyses .....  | 3-2  |
| Table 3-2 Matrix of steady state thermal cases analyzed .....   | 3-3  |
| Table 3-3 Matrix of end cap steady state thermal cases evaluated .....  | 3-4  |
| Table 4-1 Key geometric data of transient cases.....  | 4-2  |
| Table 4-2 Relevant material data for steady state thermal evaluation .....  | 4-2  |
| Table 4-3 Additional finite element cases analyzed.....   | 4-3  |
| Table 4-4 Initial thermal transient finite element results.....   | 4-5  |
| Table 4-5 All thermal transient finite element results .....  | 4-6  |



# 1 INTRODUCTION

A configuration of pipe support that has seen increasing application in recent times, particularly on main steam and hot reheat high-energy piping (that are often fabricated from Grade 91 steel), is a so-called “trunnion support” in which load is transferred from the main pipe to a hanger system through “trunnions” that are welded to the main pipe run. Some examples are shown in Figure 1-1. The term “trunnion” is used to refer to the hollow circular cross-section attachment. This “trunnion” is fabricated from a similar pipe to that of the main piping run to which it attaches (usually with a full-penetration weld) but is generally of smaller diameter and of different wall thickness to the piping run.

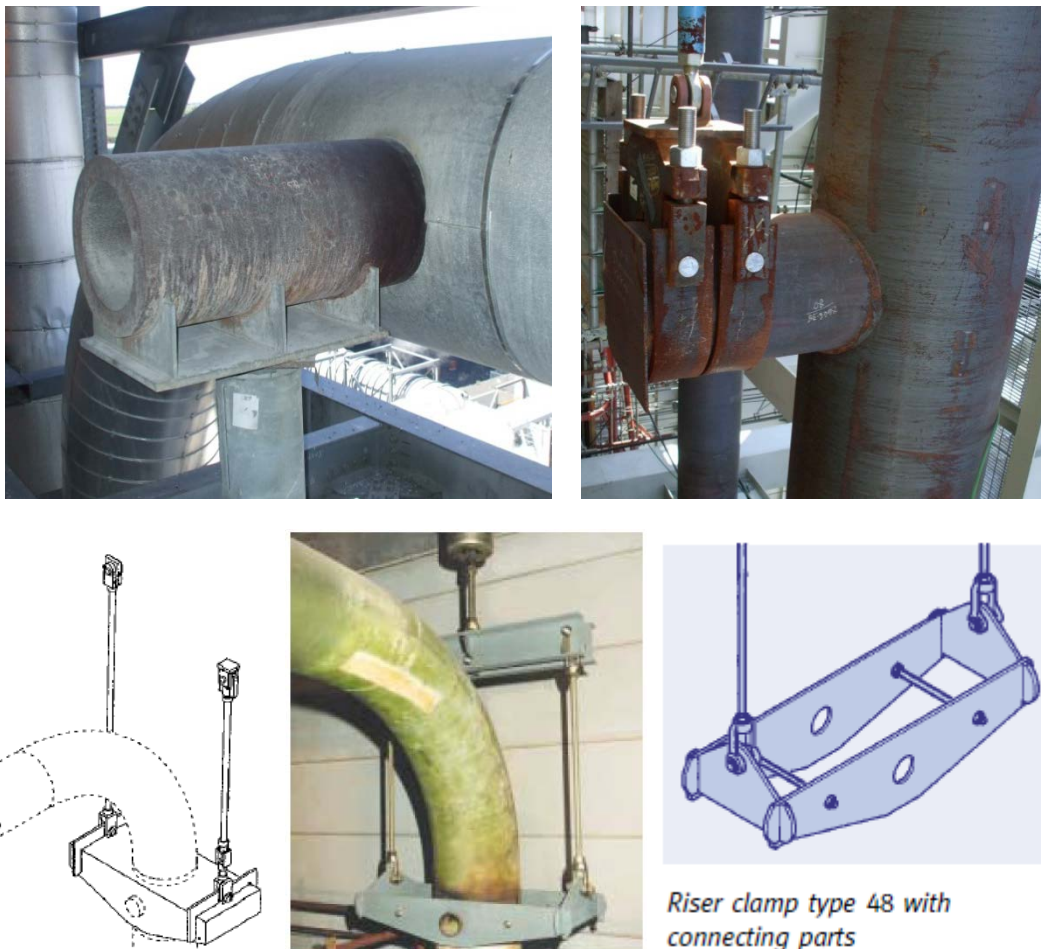


**Figure 1-1**  
Schematics of trunnions and a riser clamp arrangement that utilize trunnions welded to the main pipe run

This configuration of support has been used for many years in low temperature systems, and in petrochemical plants, but has found increasing application in the high energy piping systems of modern supercritical and combined cycle power plants. As indicated in Figure 1-1 there are several configurations that may be used with high energy piping systems, and in common with other high energy piping fabrications, questions have been raised about the need to inspect the pipe to trunnion weld. In configurations that utilize a frame that fits over the trunnion then access to the trunnion to pipe weld is restricted, thereby limiting opportunity for inspection (unless the frame or harness is dismantled). In other configurations, the riser clamp (harness) arrangement may not be present (so gaining access may be simpler – insulation removal, rather than disassembly of the support) but there are a variety of lengths of trunnion and loading magnitudes and directions so questions have been raised about the need for inspection of the trunnion to pipe weld; e.g., is this weld greater risk of damage/cracking than other welds in the piping system, even though it is not a pressure boundary?

To provide some insight into the need for inspection of the pipe to trunnion welds a series of evaluations are reported here to investigate sustained loads and temperature gradients (static and transient) that might affect the integrity of the trunnion to pipe weld. The objective is not to provide detailed analysis of all trunnion configurations but to highlight a number of the more important parameters that affect the local stresses at the trunnion to pipe weld to provide simple screening tools to identify which trunnions should be subject to more detailed analysis and/or inspection.

To limit the scope of this study, investigations are restricted to trunnions used on high energy piping systems (main steam and hot reheat) of modern utility and combined cycle plants, which are invariably fabricated from Grade 91 steel. Of specific concern for such systems is the weld between the pipe and trunnion which could be susceptible to Type IV cracking since this creep-weak zone within the heat affected zone is stressed in the so-called cross-weld direction by the loads that act on the trunnion. Strength reduction factors are progressively being introduced (e.g., in ASME Section I) to account for this weak zone, but it is unlikely that such factors were considered in trunnion design and may, therefore, represent additional risk.

The technical content of this report is separated into three principal sections to address static loading, steady state temperature distribution and transient thermal stress.

The section on static loading summarizes some of the published approaches for design of trunnions and assessment of their impact on the piping stresses. A selection of example cases is investigated with finite element analysis to highlight the influence of geometry and loading on the resulting stresses within the trunnion and pipe to which it is attached. Consideration is given to the stress magnitude relative to other stresses in the piping and the likely location and mode of damage/cracking is explored to identify whether this occurs in the pipe or in the trunnion, including susceptibility to creep damage within the Type IV region of the weldment heat affected zone. This, in turn, provides some basic criteria to assess the likely risk of cracking for particular configurations, and selection of inspection techniques and location.



The section on steady state temperatures investigates the so-called “fin-effect” of the trunnion welded to the pipe (e.g., the trunnion may act as a cooling fin protruding through the insulation and may result in a decrease in the temperature at the trunnion to pipe weld, which may reduce susceptibility to creep damage). Calculations are performed to establish the temperature at the base of the trunnion for a variety of possible configurations (e.g., insulated/uninsulated, with and without end caps) to determine if any credit can be taken for the “fin-effect”.

The section on transient thermal stress explores the effect of steam temperature changes within the piping on the thermal stresses at the pipe to trunnion weld. As the steam temperature rises, for example during a plant startup, and the steam line heats up, the temperature of the trunnion will lag behind that of the steam line due to the time taken for heat conduction to warm the trunnion. This results in a thermal stress at the base of the trunnion which is influenced by the rate of steam temperature change and by the pipe and trunnion geometry. Based on the analysis results, a simple screening criterion is proposed to help identify which trunnions are likely to be more at risk of thermal fatigue damage so that these can be prioritized for more detailed analysis and/or inspection.

In combination, the results and derived criteria for screening for various failure mechanisms provide practical tools to allow trunnions on a particular piping system, or across several piping systems, to be prioritized for more detailed evaluations and/or inspection.



# 2

## STATIC LOADING

---

The steady loading imposed at normal operating conditions is of particular interest because the main steam and hot reheat piping systems operate at temperatures where long-term creep is a possible failure mechanism. The loads supported through the trunnion develop stresses within the trunnion itself, and loads are transferred to the pipe to which it is attached thereby creating local stresses in the piping that may be additional to the hoop and axial stresses due to internal pressure or system loads. These stresses could result in:

- Enhancement of creep damage in the pipe (because the stresses are additive to those from internal pressure or other system loads).
- Creep damage in the trunnion (particularly at the weld due to creep weak Type IV region).

Specific questions that will be addressed in this section of the report include:

- How do the stress magnitudes at the trunnion compare to stresses elsewhere in the piping?
- Where is the likely location of cracking – within the trunnion, or can damage propagate into the piping?
- Is accelerated creep damage likely in the piping in the vicinity of the trunnion?
- What inspection techniques should be applied to find possible damage?

Before investigating the mechanical integrity of the trunnion attachments to address these questions the design rules and codes that are relevant to trunnion type attachments are explored.

### 2.1 Design Rules and Codes

The majority of piping systems for utility and combined cycle plants within the USA, and many internationally are designed in accordance with the requirements of ASME B31.1 (Power Piping) [1]. This design Code provides rules and guidance for high energy piping systems but does not explicitly include methods to calculate local stresses at trunnion type attachments. Therefore, the designer must draw on information from other sources. Pipe support manufacturer's catalogues [2] are frequently used to select standard pipe supports from pre-determined sizes. Such catalogues are available for supports that can be connected to a piping system by means of a trunnion, but the catalogues do not include specific information to size the trunnion or to determine if the local stresses imposed on the piping are acceptable.

Historically there have been a number of approaches to the sizing of trunnions and calculation of their effect on the local piping stresses. Perhaps the most widely referenced (and possibly widely used) approach is that documented by M.W. Kellogg Company [3]. This method basically assumes that the trunnion applies an axisymmetric load to the pipe and the resulting stresses in the pipe are determined from the governing equation for a beam on an elastic foundation, with the inherent assumptions associated with thin shell theory (henceforth, this method will be

referred to as the Timoshenko method). Hence, although there is no validity limit specified in the approach documented by M.W. Kellogg Company [3], the method is strictly only applicable to thin shells ( $D/t > 20$ ) and for cases where the trunnion is small compared to the pipe ( $d/D < 0.5$ ).

In simple terms, this Timoshenko method leads to the following equation for the bending stress induced in the pipe by a load per unit circumference (F) created by the loading on the trunnion.

$$\sigma_B = \frac{1.17F\sqrt{R}}{T^{1.5}}.$$

Where R is the outer radius of the pipe run and T is the thickness of the pipe run. The load per unit circumference, F, can be computed for various loads on the trunnion. For the case of a bending load then:

$$F = \frac{M}{\pi r^2}.$$

Where M is the bending moment resulting at the pipe to trunnion connection and r is the outer radius of the trunnion.

When calculating the total stress in the pipe (due to the inherent piping stress and the effect of the trunnion), consideration must be given to the orientation of the loading on the trunnion relative to the orientation of the pipe, as illustrated in Figure 2-1. Specifically, if the bending is “in-plane” then an estimate of the total stress in the pipe can be obtained by summing the bending stress induced in the pipe by the trunnion (calculated per above equation) and the axial stress in the pipe (due to pressure and other system loads). If the bending is “out-of-plane” then an estimate of the total stress in the pipe can be obtained by summing the bending stress induced in the pipe by the trunnion (calculated per above equation) and the hoop stress in the pipe (due to pressure).

Because it is generally the case that the wall thickness of the pipe is designed based on the hoop stress due to pressure alone, it is generally preferred not to have an “out-of-plane” bending configuration for the trunnion loading. This is borne out by an ad-hoc survey of a few power plant projects that employ trunnion supports – the vast majority follows the preferred “in-plane” configuration. Indeed, from the perspective of identifying trunnion supports that might be “at risk” then “out-of-plane” loading represents a key factor.

Beyond the Timoshenko method, other approaches have been followed to develop solutions for the pipe to trunnion configurations based on other elasticity approaches as well as more empirical approaches. Documents such as WRC Bulletin 107 [4] discuss such approaches and provide associated calculations. This method is frequently referenced in the technical literature, but the breadth of its use in practical piping design is not known.

A comparison of the stress predictions from the Timoshenko method and the WRC Bulletin 107, for a variety of pipe and trunnion sizes is provided by Bhattacharya [5]. The basic conclusions from that work is that the WRC107 calculation may result in stresses that are higher or lower compared to detailed finite element simulations (the degree of error being greater than 100% in some cases). The Timoshenko method is described as being “not grossly incorrect, as long as the load is not a radial one where stresses are significantly under predicted”. Hence, for trunnions that are predominantly loaded in bending, then the Timoshenko method is likely a prudent approach.

Yet other approaches for trunnion design adopt solutions for nozzles in piping systems with external forces and moments applied to the nozzle. Such solutions are generally of limited applicability because they assume that internal pressure in the pipe run also acts in the nozzle (whereas the trunnion does not experience such internal pressure) and they inherently neglect the reinforcement provided by the contiguous pipe (since no hole is bored in the pipe for a nozzle; the trunnion is simply welded to the outside of the pipe). Thus such approaches are not explored further in this report.

The ASME Nuclear Code (Section III) includes, in the appendices, a “procedure for evaluation of the design of hollow circular cross-section welded attachments on piping.” There are two relevant articles, Article Y-4000 for Class 1 piping and Article Y-5000 for Class 2 and 3 piping [11]. Note that prior to the 2010 edition of the code, these articles were in the form of Code Cases [6][7]. The principal difference between the two Articles is that the calculations for Class 1 piping include effects of thermal stresses (due to pipe to trunnion temperature difference) whereas the calculations for Class 2 and 3 piping do not. The basic approach of these Articles is to use corrections to the calculated bending, normal and shear stress in the trunnion to estimate the stress in the pipe. In all cases the correction factor can be no less than unity; that is the stress induced in the pipe by the trunnion cannot be less than the calculated stress in the trunnion (this represents quite a conservative assumption for some cases).

The basic method of the ASME Code Articles is summarized below, with simplification for one loading direction that causes bending in the trunnion. The article contains a number of geometric criteria that must be satisfied for use of the method, specifically:

$$4.0 \leq \frac{D}{2T} \leq 50.0,$$

$$0.2 \leq \frac{t}{T} \leq 1.0,$$

$$0.3 \leq \frac{d}{D} \leq 1.0.$$

The induced stress in the pipe by the trunnion is then calculated from:

$$S_{MT} = \frac{4 B M r}{\pi\{r^4 - (r-t)^4\}} + \frac{2 Q}{\pi\{r^2 - (r-t)^2\}}.$$

Where M is the applied bending moment, Q is the shear load at the pipe to trunnion connection and B is a coefficient that depends on geometry and loading orientation, and has the form:

$$B = 0.5A_o \left(\frac{D}{T}\right)^{n_1} \left(\frac{d}{D}\right)^{n_2} \left(\frac{t}{T}\right)^{n_3},$$

Where  $A_o$ ,  $n_1$ ,  $n_2$ ,  $n_3$  are coefficients documented in the Code Article. The parameter B is not permitted to be less than unity, which results in the stress in the pipe being equal to the combined bending and shear stress in the trunnion.

This stress in the pipe due to the trunnion is then added to the other axial stresses in the pipe (due to pressure or other system loads) for assessment against the material allowable stress. The Code does not specifically address addition to hoop or axial stress based on the orientation of the loading on the trunnion (although the coefficients involved in the calculation of B differ for in-plane and out-of-plane loading).

Essentially the same approach as that used in the ASME Nuclear Code Articles is employed in the European Norm for design of piping systems, EN13480-3 [8]. The approach is documented in Clause 11.3 but is not discussed further here due to its similarity to the ASME Code Article approach.

The approach in the ASME Articles (and by inference the EN Code) was reviewed and assessed against available experimental data as part of another EPRI study [9]. That work concluded that the stress estimations were conservative, typically by a factor of approximately 1.5. Such factors of conservatism are large for components operating in the creep range because the creep life is approximately related to the 5<sup>th</sup> power of the applied stress; hence if the stress is conservative by a factor of 1.5 then the creep life will be conservative by a factor of approximately 7.6. Therefore, the approach documented in the ASME Articles (and EN Code) is likely conservative for design purposes. However, the high level of conservatism could result in undue concern for lifetime of components operating in the creep range. Moreover, because of the conservative use of a correction factor that ensures that the induced stress in the pipe is no less than the total stress in the trunnion, it is possible that use of this method could result in a ranking of damage likelihood that is not consistent with the actual risk of damage.

To better assess the actual margins and ranking capabilities of these stress calculation methods the next sections provide detailed comparisons for the cases of in-plane and out-of-plane loading, respectively.

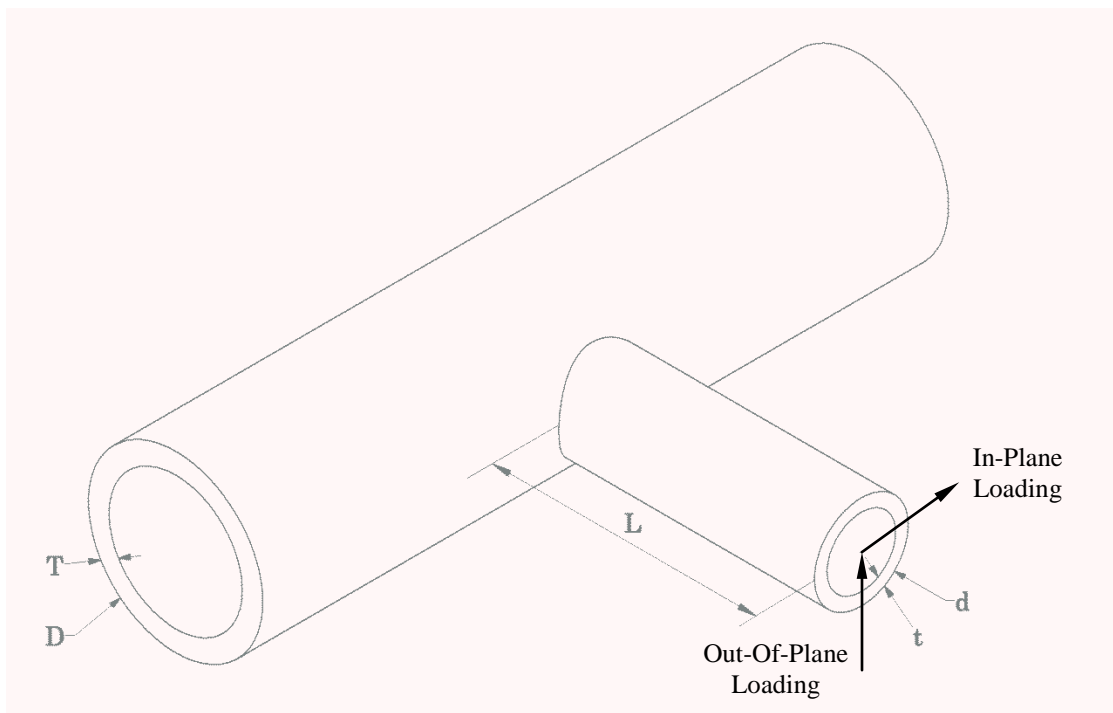


**Figure 2-1**  
General configuration of a pipe with a trunnion illustrating the directions of in-plane and out-of-plane loading

## 2.2 Trunnions with In-Plane Loading

To provide an indication of the typical stress levels caused by trunnions a sample of trunnion configurations from actual Grade 91 piping systems has been collected. The range of configurations is not intended to cover all possible variables, but rather represents an ad-hoc sampling of configurations from actual projects. The different configurations are summarized in Table 2-1. These cases include trunnions from main-steam and hot reheat systems, and cases of relatively short trunnions that are used in conjunction with a riser clamp arrangement, and cases of longer trunnions braced to some other support steel. In all cases the trunnions produce loading in an “in-plane” configuration.

The stresses calculated for these different trunnion configurations are summarized in Table 2-2. The table provides validity checks against the ASME Article geometric criteria, from which it can be seen that the majority of cases do not meet the validity check for the ratio of trunnion thickness to pipe thickness ( $t/T$ ). Nevertheless, the ASME Article calculation is followed to estimate the stress that would be added to the normally calculated piping stress. Also calculated is the local stress in the pipe due to the trunnion estimated by the Timoshenko method. For completeness, the stresses in trunnion are also reported (both the bending and shear stress at the junction to the pipe). In the majority of cases because the correction factor (B) determined from the ASME Article is unity, then the ASME Article calculated stress is simply the sum of the bending and shear stress calculated for the trunnion.

It is evident that the stresses calculated by the Timoshenko and ASME methods are significantly different in a number of cases, for example Cases 4 and 6 for short trunnions where the shear stress is larger than the bending stress. In these cases the Timoshenko method is only considering the bending stress component, which is a small contribution. In all but Case 5, the ASME method provides a higher, or significantly higher, stress estimate than the Timoshenko method.

The bending and shear stress in the trunnion are also reported in Table 2-2. These are of interest, particularly for Grade 91 piping systems because the weld between the pipe and the trunnion will create a heat affected zone (and accompanying creep-weak type IV zone) that could be vulnerable to creep failure with a sustained load. The bending stress magnitudes in the trunnion (which would act on the type IV zone of the trunnion to pipe weldment) are in all cases less than half the allowable stress for the Grade 91 material at the design temperature. Given that the strength reduction factor for the type IV zone of a Grade 91 weldment is not less than 0.5, then the trunnion stresses do not appear to be sufficiently large to cause concern for premature type IV creep damage or cracking at the trunnion to pipe weld.

Hence concern turns to the enhancement of stress in the Grade 91 piping and the effect that this may have on the longevity of the pipe. Because of the approximating assumptions of both the ASME and Timoshenko methods it is not immediately clear which method provides the more accurate estimate of stress. Therefore, the cases have been analyzed using a simple finite element model to give a more realistic estimate of the actual stress in the pipe due to the loading from the trunnion. This model, which is shown in Figure 2-2, includes the trunnion and a portion of the pipe to which it attaches. Only half of the pipe (one side with the trunnion) is modeled due to the inherent symmetry. The load on the trunnion is applied as a distributed traction at the end of the trunnion. Only the trunnion load is considered; no internal pressure or other system loads are applied to the pipe such that the stresses are purely those due to the trunnion and associated loads (to facilitate comparison with the stress calculated by the other methods). The pipe to trunnion

junction (where the weld would be) does not consider the weld detail; that is, the trunnion cross-section is connected directly to the outside surface of the pipe. This creates a stress singularity so the local stresses are very sensitive to the element size of the finite element mesh. To overcome this, the through-wall stress in the trunnion is linearized to a membrane and bending component which facilitates comparison with the Timoshenko and ASME results. A typical axial stress distribution within the pipe run is shown in Figure 2-3, where it is evident that the trunnion loading creates a bending stress through the wall of the pipe. This through-wall stress distribution (from the side of the trunnion that places the outside diameter of the pipe in tension), and the stress linearization, is shown in Figure 2-4.

The results of these analyses are summarized in Table 2-3 which provides the calculated (linearized) bending stress in the pipe, and also lists the stresses from the ASME and Timoshenko methods (repeated from Table 2-2 to facilitate comparisons). In general, the Timoshenko method provides stress estimates that are in better agreement (with slight conservatism) with the finite element results than the ASME methods, with the largest deviation being Case 5, which was the only case where the Timoshenko method was more conservative than the ASME method.

The magnitude of the stress induced in the pipe by the trunnion is quite modest with the greatest stress being 5.8ksi for Case 5. It is noted that this is an elastically calculated stress so it does not account for the stress redistribution that would occur due to creep (which would tend to relax the higher stresses). Even so, the stress magnitude is small compared to the allowable stress at the design temperature (approximately 13ksi). Therefore, it would appear that the rules that were applied for trunnion design in the cases analyzed here, that the stress magnitudes are within reasonable limits that would not cause concern for premature failure of either the trunnion (due to its inherent bending stress combined with the weakness associated with the type IV zone of the weldment) or in the pipe (due to the induced stress which is reasonably estimated by the Timoshenko method and which when combined with the axial stress due to pressure (conservatively estimated as half the allowable stress) does not exceed the material allowable.

**Table 2-1**  
**Sample of trunnion configurations from actual piping systems (all with in-plane loading)**

| Case | Temp | Pressure | Pipe O.D. | Pipe Thk. | Trunnion O.D. | Trunnion Thk. | Load  | Moment Arm |
|------|------|----------|-----------|-----------|---------------|---------------|-------|------------|
|      | (F)  | (psi)    | (in)      | (in)      | (in)          | (in)          | (lb)  | (in)       |
| 1    | 1065 | 3970     | 20        | 2.7       | 16.0          | 1.6           | 48000 | 27.9       |
| 2    | 1065 | 3970     | 20        | 2.7       | 14.0          | 1.4           | 30250 | 18.3       |
| 3    | 1065 | 3890     | 24.75     | 3.4       | 14.0          | 0.8           | 35000 | 19.6       |
| 4    | 1065 | 3890     | 24.75     | 3.4       | 12.75         | 0.5           | 38742 | 2.8        |
| 5    | 1065 | 780      | 40        | 1.3       | 20.0          | 0.8           | 31400 | 25.0       |
| 6    | 1065 | 3890     | 18.86     | 2.4       | 8.6           | 0.5           | 20554 | 2.3        |
| 7    | 1090 | 805      | 32.39     | 1.2       | 10.8          | 0.5           | 32027 | 3.7        |



**Table 2-2**  
**Calculations of stress in trunnion and pipe for sample trunnion configurations using the stress calculations methods of Timoshenko and ASME article**

| Case | ASME Article Validity Checks |       |                          |       |                          |       | ASME Article Stress Correction Factor |                |                |                | Trunnion Stresses |           | ASME Article | Timoshenko  |
|------|------------------------------|-------|--------------------------|-------|--------------------------|-------|---------------------------------------|----------------|----------------|----------------|-------------------|-----------|--------------|-------------|
|      | <input type="checkbox"/>     | Valid | <input type="checkbox"/> | Valid | <input type="checkbox"/> | Valid | C <sub>L</sub>                        | C <sub>L</sub> | C <sub>L</sub> | B <sub>L</sub> | Bending           | 2 x Shear | Pipe Stress  | Pipe Stress |
|      |                              |       |                          |       |                          |       | Pipe                                  | Attach         | Overall        |                | (ksi)             | (ksi)     | (ksi)        | (ksi)       |
| 1    | 3.68                         | X     | 0.59                     | Y     | 0.80                     | Y     | 0.97                                  | 1.55           | 1.55           | 1.00           | 5.7               | 1.3       | 7.0          | 5.5         |
| 2    | 3.68                         | X     | 0.52                     | Y     | 0.70                     | Y     | 0.88                                  | 1.55           | 1.55           | 1.00           | 3.5               | 1.1       | 4.5          | 3.0         |
| 3    | 3.67                         | X     | 0.22                     | Y     | 0.57                     | Y     | 0.43                                  | 1.22           | 1.22           | 1.00           | 7.0               | 2.2       | 9.2          | 3.0         |
| 4    | 3.67                         | X     | 0.15                     | X     | 0.52                     | Y     | 0.30                                  | 1.08           | 1.08           | 1.00           | 1.9               | 4.0       | 5.9          | 0.6         |
| 5    | 15.8                         | Y     | 0.64                     | Y     | 0.50                     | Y     | 2.57                                  | 2.68           | 2.68           | 1.34           | 3.5               | 1.3       | 5.9          | 9.2         |
| 6    | 3.88                         | X     | 0.21                     | Y     | 0.46                     | Y     | 0.42                                  | 1.30           | 1.30           | 1.00           | 1.9               | 3.2       | 5.1          | 0.8         |
| 7    | 13.5                         | Y     | 0.42                     | Y     | 0.33                     | Y     | 1.64                                  | 2.56           | 2.56           | 1.28           | 3.0               | 4.0       | 7.8          | 4.6         |

**Table 2-3**  
**Comparison of calculations for stress in the pipe created by the loading from the trunnion**

| Case | ASME Article | Timoshenko | FEA    |
|------|--------------|------------|--------|
|      | Stress       | Stress     | Stress |
|      | (ksi)        | (ksi)      | (ksi)  |
| 1    | 7.0          | 5.5        | 4.2    |
| 2    | 4.5          | 3.0        | 2.4    |
| 3    | 9.2          | 3.0        | 2.6    |
| 4    | 5.9          | 0.6        | 0.8    |
| 5    | 5.9          | 9.2        | 5.8    |
| 6    | 5.1          | 0.8        | 1.2    |
| 7    | 7.8          | 4.6        | 4.5    |

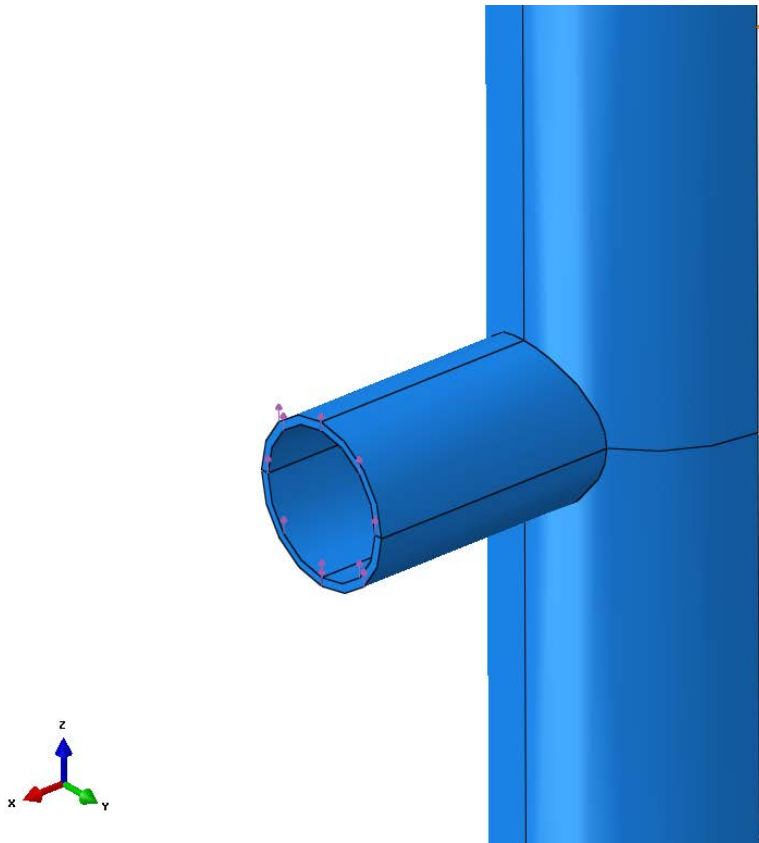


**Figure 2-2**  
**Model of pipe and trunnion for analysis of static stresses (Case 3)**

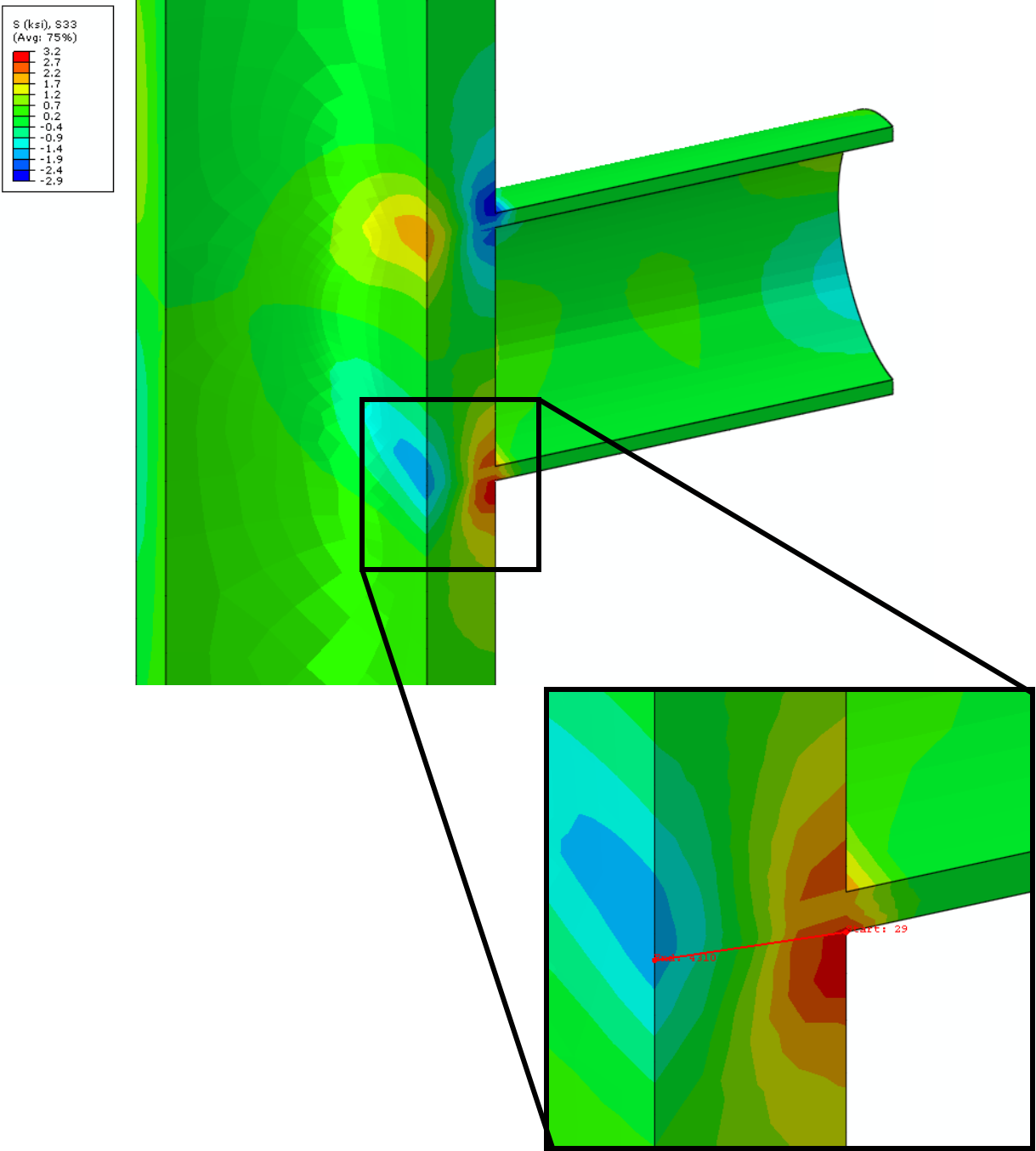


**Figure 2-3**  
Cut-away view showing a color contour plot of the axial stress distribution in the pipe and trunnion (Case 3)

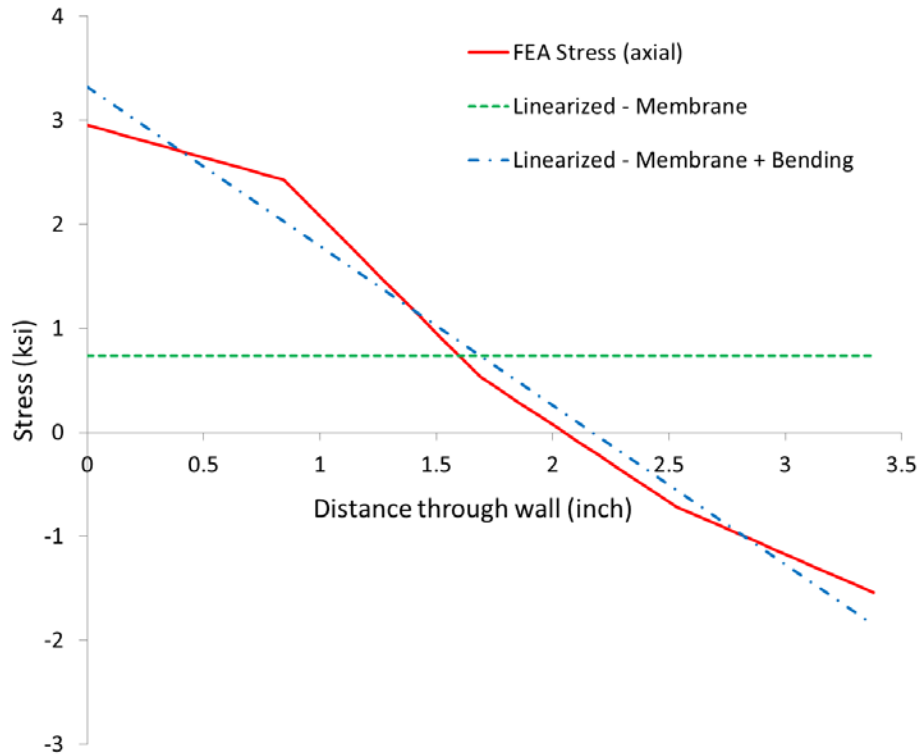


**Figure 2-4**  
**Distribution of stress in the pipe, and linearization to provide a stress to compare with ASME Code article and Timoshenko methods (Case 3)**

### 2.3 Trunnions with Out-Of-Plane Loading

Of the examples of trunnions reviewed from actual plants, it appears that out-of-plane loading is less common but can be used in some cases (e.g., support of a horizontal pipe run with trunnions welded on each side of the pipe). To explore the significance of this mode of loading compared to the in-plane loading examined in the previous subsection, the same set of cases has been used but with the pipe orientation/loading direction changed to represent an out of plane load. It should be recognized that these cases were not designed as out-of-plane loading scenarios, but they do provide a relative comparison of stress magnitude for the same geometry and load with only the loading direction changed.

To determine the stresses, the previous finite element models (from the in-plane loading analyses) were used with the direction of loading changed to represent an out-of-plane scenario (again, only the loading on the trunnion was applied; that is no additional loads such as pressure within the pipe were considered – that facilitates comparison with analytical solutions for the stress induced in the pipe by the trunnion). Figure 2-5 shows a typical stress distribution for out-of-plane loading. As for the in-plane loading scenario, the bending stress through the wall of the pipe was determined using stress linearization along a (now radial) stress categorization line (also illustrated in Figure 2-5). The resulting through-wall stress distribution and linearized stresses are shown in Figure 2-6.

The results for each of the seven cases are summarized in Table 2-4, which documents the (linearized) bending stress calculated from the finite element model and the stress estimated from the Timoshenko method (which is identical to the in-plane loading cases because the method makes no distinction between loading direction). The calculated bending stresses in several cases are higher for out-of-plane loading than for in-plane loading, most notably Case 5 where the linearized bending stress is approximately double that for in-plane loading and now exceeds the stress estimated by the Timoshenko method. This case involves a relatively thin reheat pipe with a high loading on the trunnion; this would not be permissible in practice (with out-of-plane loading) but serves to highlight that the Timoshenko method provides a reasonably accurate estimate of stress (at least for ranking purposes). More generally the Timoshenko method provides a reasonable stress estimate (of appropriate magnitude compared to the finite element results) and therefore represents an apparently effective tool for design of trunnions on piping systems for either in-plane or out-of-plane loading. Indeed, the accuracy of this method is quite surprising given its simplicity and the diversity of dimensions in the cases considered (which are often beyond the reasonable proportions associated with the underlying thin-shell theory). However, these comparisons provide confidence in general application of this method for design and for identifying trunnions that have higher loading and which may have greater susceptibility to cracking.

Indeed, since the basic design approach for out-of-plane loading is to perform linear superposition of the hoop stress in the pipe and the stress induced in the pipe by the trunnion then a conservative design will inevitably result because this approach does not account for the beneficial redistribution of stress that would occur due to creep (both across the region with the maximum bending stress, and from that region to the surrounding portions of the pipe).

The next section considers the implications of these results for in-plane and out-of-plane loading with regard to likely modes of failure and location of damage.

**Table 2-4**  
**Comparison of calculations for stress in the pipe created by the loading from the trunnion**

|      | Timoshenko | FEA    |
|------|------------|--------|
| Case | Stress     | Stress |
|      | (ksi)      | (ksi)  |
| 1    | 5.5        | 5.5    |
| 2    | 3.0        | 1.8    |
| 3    | 3.0        | 3.3    |
| 4    | 0.6        | 1.0    |
| 5    | 9.2        | 13.3   |
| 6    | 0.8        | 1.1    |
| 7    | 4.6        | 6.2    |

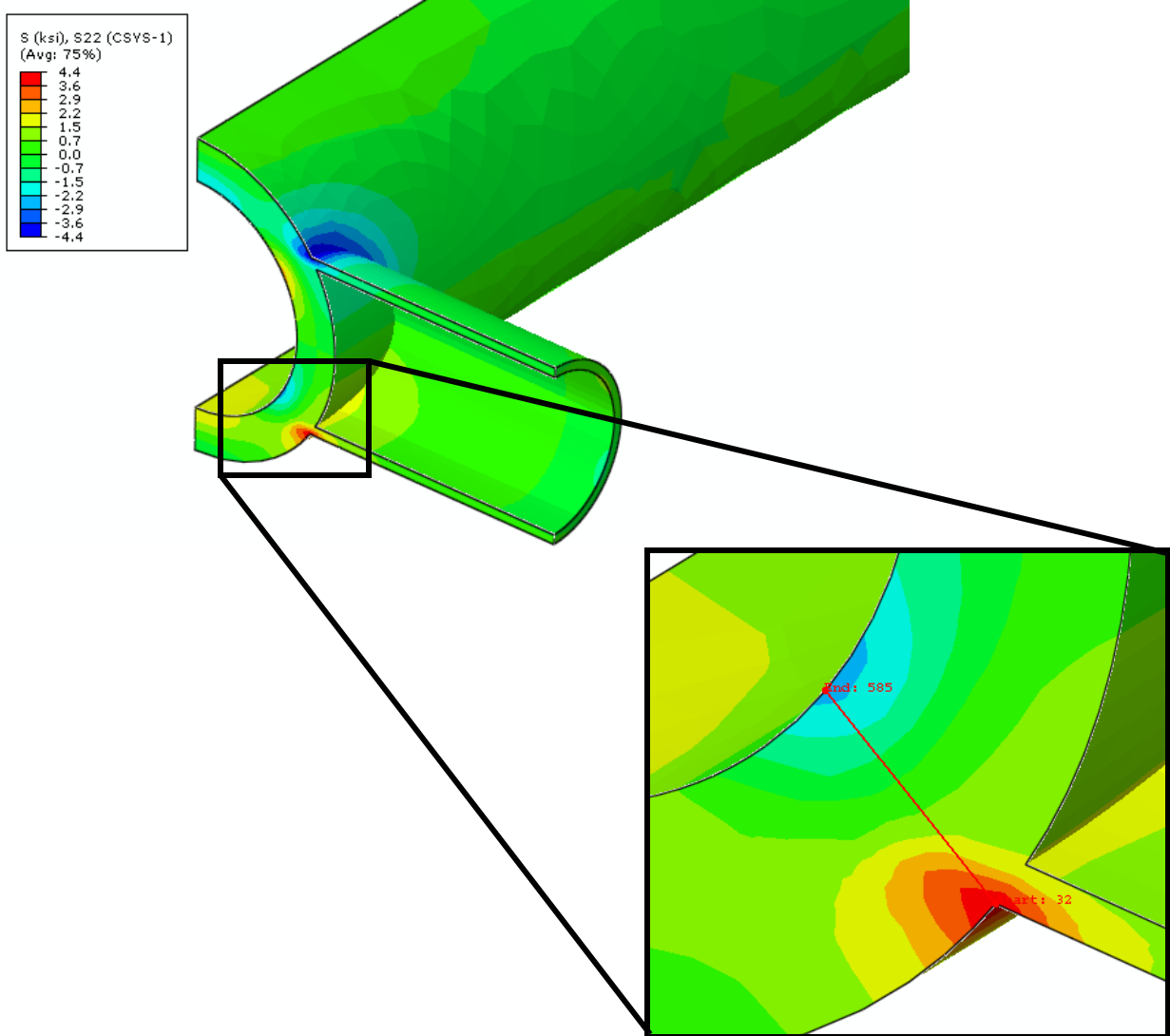
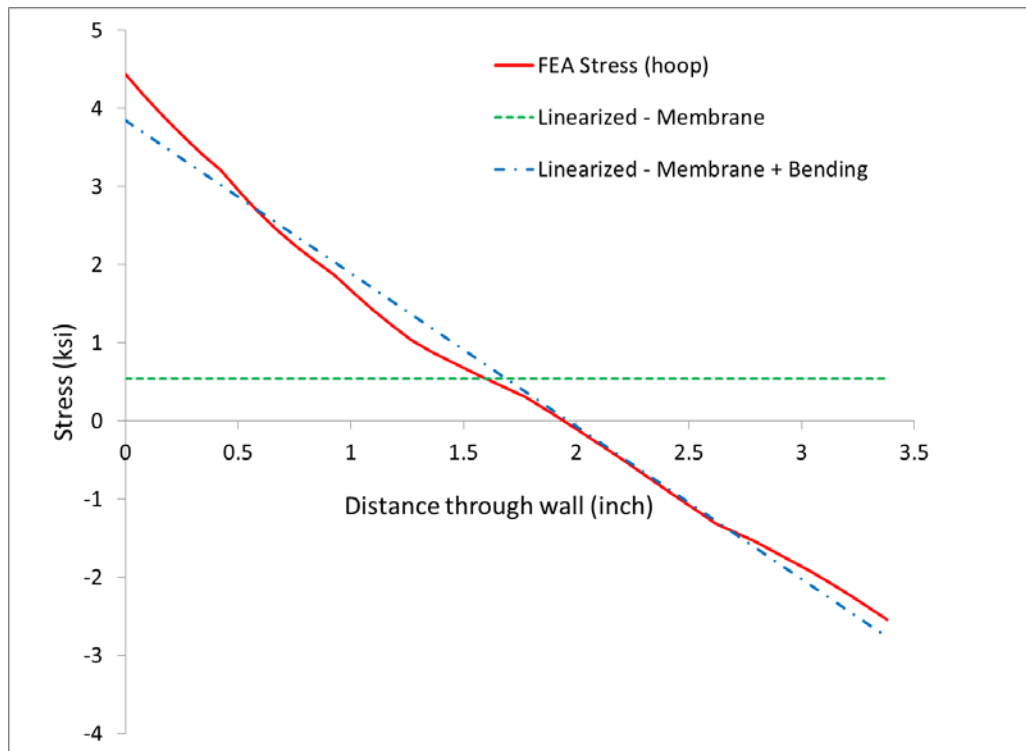


Figure 2-5  
Cut-away view showing a color contour plot of the hoop stress distribution in the pipe and trunnion (Case 3)



**Figure 2-6**  
**Distribution of hoop stress in the pipe, and linearization to provide a stress to compare with Timoshenko method (Case 3)**

## 2.4 Stress Distribution and Susceptibility to Type IV Cracking

From the preceding analysis results, particularly with the visualization of stress distributions from the finite element analyses, some general observations can be made about the likely susceptible locations for damage based on the applied load and geometry. This is of particular interest because for trunnions used in main-steam and hot reheat systems the pipe and trunnion are usually fabricated from Grade 91 (or some other creep strength enhanced ferritic steel); welding of the trunnion to the pipe will result in heat affected zones being formed on the trunnion and pipe sides of the weld deposit and it is known that a creep-weak zone, commonly referred to as the type IV region, will exist within the heat affected zone. This type IV region is generally quite susceptible to creep damage when the loading is applied directly across this region (so-called cross-weld direction). Therefore, these type IV regions will be susceptible to creep damage for cases of high bending stress within the trunnion (which will apply a cross-weld stress), for both in-plane and out-of-plane loading. For cases where higher stresses are induced in pipe (e.g., out of plane loading) then type IV cracking could initiate at the type IV zone on the pipe side of the weld deposit, but the orientation of the heat affected zone and overall stress distribution suggests that growth of creep damage to cause failure (at least if just due to sustained loading) is unlikely. Nevertheless, if more detailed evaluations suggest susceptibility to creep damage initiation, further investigation should be performed to confirm that the damage will not propagate to cause failure of the pipe to trunnion weld. Figure 2-7 summarizes some of these considerations that control susceptibility to the likely location for damage initiation or failure.

The potential for cracking at the saddle of the trunnion is highlighted by several examples (such as shown in Figure 2-8) of premature creep-cracks being identified at nozzle (and weldolet) connections in Grade 91 headers and piping (with predominantly internal pressure loading; that is little or no external force or moment applied to the nozzle). In the majority of these cases, the creep damage has been localized to the surface region within the type IV zone of the weldment and does not immediately threaten the overall integrity or load bearing capacity of the connection. Based on this experience, then the saddle region of a trunnion connection may be a location for preferential damage (particularly if the trunnion provides substantial reinforcement to the pipe), even if the loading applied to the trunnion is such that the stresses in the trunnion or pipe are small.

To further illustrate this effect, Figure 2-9 shows a plot of the accumulated equivalent creep strain from a steady-state creep analysis with no load applied to the trunnion (internal pressure only within the pipe). This plot highlights that although there is no load applied to the trunnion there is a concentration of creep strain at the saddle location of the pipe-to-trunnion connection. While the creep strain magnitude is no higher than that on the internal surface of the pipe, there may in practice be some preferential creep strain accumulation within the type IV region of the weld boundary in the pipe (the analysis results presented here assume homogeneous, base metal, properties for the pipe and trunnion; the weldment is not modeled).

The possible damage locations and influence factors described here can be used in conjunction with estimates of stress at the base of the trunnion (bending and shear in the trunnion to pipe weld) and with estimates of stress induced in the pipe (using the Timoshenko method) and the nominal hoop and axial stresses in the pipe to which the induced stress in the pipe is added, depending on the plane of loading for the trunnion. The resulting stress magnitudes provide a reasonable basis for ranking trunnions within a piping system for damage susceptibility and identifying the likely location of damage for a particular trunnion. However, the stress estimates obtained with this approach are not suitable for lifetime calculations because they are generally quite conservative because they do not account for the stress redistribution that will occur due to creep (particularly of through-wall bending stress). Hence for cases screened as “high-risk” it is recommended that a more detailed finite element creep redistribution analysis be performed to provide stresses for a more realistic a life estimate that could be used to help define inspection intervals.



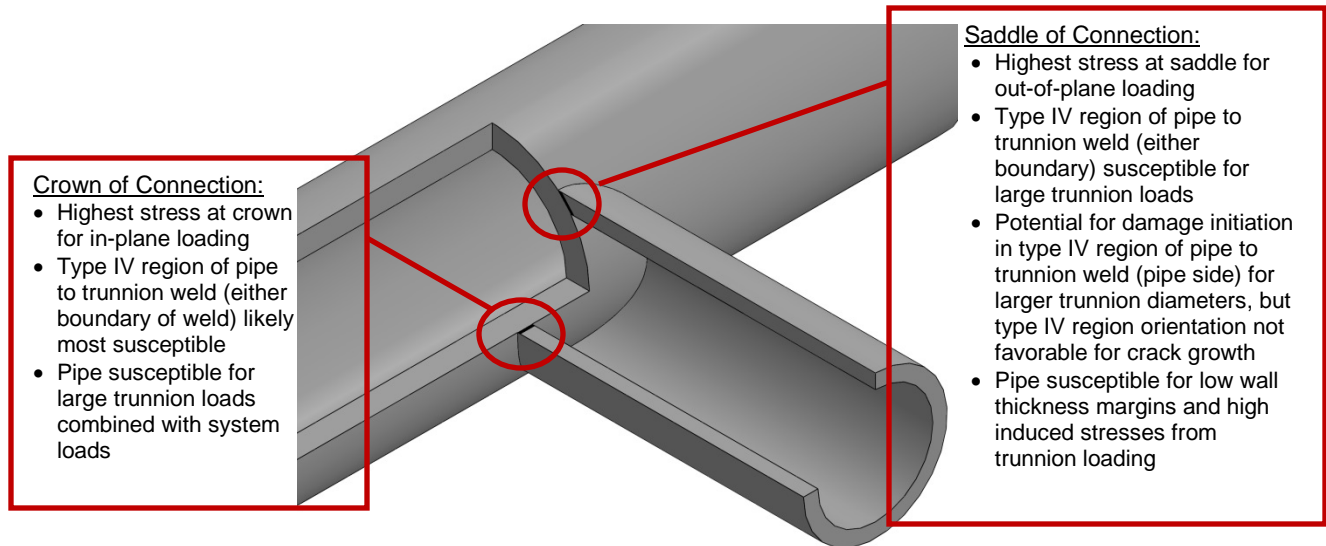


**Figure 2-7**  
Cut-away view of trunnion to pipe connection with annotation to indicate likely location of damage for different loading scenarios

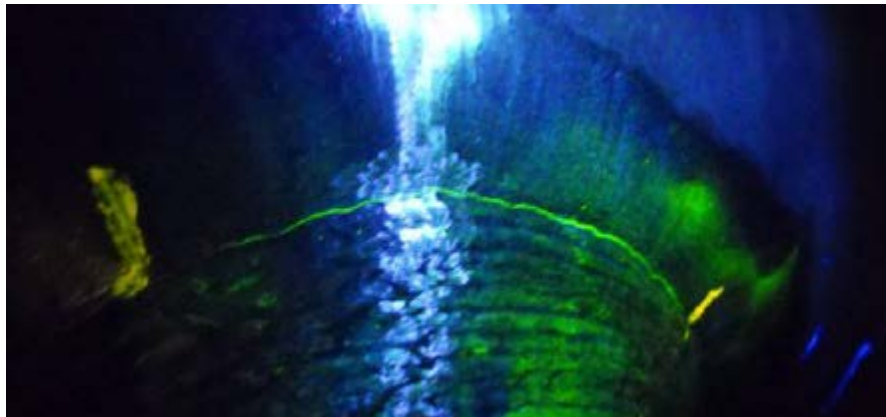


**Figure 2-8**  
Photograph of a Type IV crack at the saddle of a nozzle connection in a Grade 91 piping system

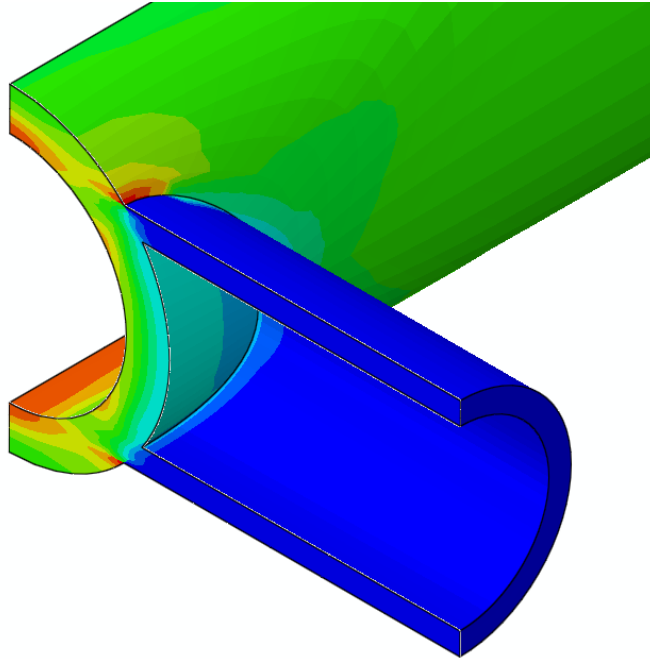


**Figure 2-9**  
Color contour plot showing the spatial distribution of equivalent accumulated creep strain from a steady state creep analysis with no load applied to the trunnion (internal pressure only)

## 2.5 Conclusions from Static Loading Analysis

The analyses demonstrate that under static loading trunnions subjected to out-of-plane loading are likely to represent a higher risk (susceptibility to creep damage formation) than trunnions subjected to in-plane loading. The key reason for this is that out-of-plane loading creates stresses that are additive to the hoop stress in the pipe and therefore represent a greater risk, particularly if the wall thickness of the pipe does not have much margin beyond that required to sustain the internal pressure.

However, it has also been demonstrated that even if the trunnion load is small (whether in-plane or out-of-plane) then, under creep conditions, a strain concentration can develop at the saddle of the trunnion. This is more likely to occur when the trunnion diameter or thickness are a large fraction of that of the pipe to which it is attached.

Comparison of finite element estimates of stresses induced in the pipe from in-plane and out-of-plane bending loads applied to trunnions has highlighted some discrepancies (or at least the significant conservatism) of simple calculation methods, particularly such as those employed within ASME Articles Y-4000 and Y-5000 (or the similar method within EN13480-3). The somewhat simpler Timoshenko method was demonstrated to provide better discrimination of the stress in the various cases (although not as conservative as the other methods) and is therefore judged to be suitable for use in estimating the stress induced in the pipe by the trunnion loading (at least for trunnions subjected predominantly to bending loads). Therefore this method is recommended for use in ranking the relative susceptibility of trunnions (and the pipe to which they are connected) to creep damage from sustained loading.

Hence the following overall stress ranking methodology is proposed (illustrated here for the simple case of a single load on the trunnion in either in-plane or out-of-plane direction resulting in a bending moment,  $M$ , at the pipe to trunnion connection):

1. Estimate the bending stress at the base of the trunnion (connection to pipe)

$$\sigma_{B,trunnion} = \frac{4Mr}{\pi\{r^4 - (r-2t)^4\}}.$$

2. Estimate the induced bending stress in the pipe

$$\sigma_{B,pipe} = \frac{1.17M\sqrt{R}}{\pi r^2 T^{1.5}}.$$

3. Estimate the total stress in the pipe (bending plus other stresses)

- a. In-plane:  $\sigma_{pipe,IP} = \sigma_{axial} + \sigma_{B,pipe}$

- b. Out-of-plane:  $\sigma_{pipe,OP} = \sigma_{hoop} + \sigma_{B,pipe}$

The estimated stress magnitudes can be used to rank the relative susceptibility of trunnions to damage, and hence identify which should be prioritized for inspection to identify any evidence of actual damage/degradation and/or further analysis to provide more accurate stresses and potentially lifetime estimates to develop an appropriate inspection interval. It is noted that the simplified stress estimates used for ranking are, in general, not suitable for life estimates because of their approximate nature, which when combined with typical stress exponents for creep-rupture time, would likely result in very substantial inaccuracies in estimated times for creep damage development or failure.

However, to gain some insight into the overall susceptibility for failure, the calculated stress magnitudes can be compared with, in the case of the stresses in the pipe with the material allowable stress and, in the case of stresses in the trunnion with half the material allowable stress (for Grade 91, or similar creep strength enhanced ferritics) to conservatively account for the type IV region of the pipe to trunnion weld which is stressed in the cross-weld orientation by the bending stress in the trunnion.



# 3

## STEADY STATE TEMPERATURES

---

When trunnions are used as supports then some, or all, of the trunnions may be insulated. For example, in some cases a portion of the trunnion is insulated because it is embedded in the insulation associated with the pipe to which it is attached. When the trunnion is partially insulated, heat conduction can occur through the trunnion which may result in the trunnion to pipe junction operating at a lower temperature than the nominal steam temperature in the pipe. Since creep lifetime is very sensitive to temperature then even a few degrees of temperature reduction could result in a lower risk of creep damage at the pipe to trunnion weld. To explore the significance of this effect a series of steady state heat transfer analyses have been performed for typical pipe and trunnion geometries, with different insulation scenarios and different thermal boundary conditions. The subsequent sub-sections explain the analysis method, results and conclusions.

The analyses in this section refer to steady operating conditions for which a steady state temperature distribution is established; as would be typical for periods of prolonged operation at a steady plant load. Thermal transients, in which the rate of heating (temperature rise) affects the temperature distribution, and consequently thermal stresses, are considered in a later section of this report.

### 3.1 Thermal Analysis Model

To allow a variety of pipe, trunnion and insulation configurations to be studied a parametric finite element model for the matrix of pipe and trunnion dimensions is documented in Table 3.1. The range of geometries selected bounds typical configurations for main-steam and hot reheat piping systems of utility and combined cycle plants. From review of typical trunnion configurations there is substantial variability in trunnion length depending on the style of support; e.g., trunnions used with a hanger system such as the Lisega type 48 riser clamp are short and therefore invariably buried in insulation. Longer trunnions are present when they are connected to, or supported by, other support steel. The trunnion length selected for this study allows simulation for a typical trunnion that would protrude through the insulation associated with the piping system to which it is attached.

**Table 3-1**  
**Key geometric data for steady state heat transfer analyses**

| Case | Pipe O.D. (in) | Pipe Thickness (in) | Trunnion O.D. (in) | Trunnion Thickness (in) | Trunnion Length (in) |
|------|----------------|---------------------|--------------------|-------------------------|----------------------|
| 1    | 24             | 4.1                 | 6.63               | 0.3                     | 16                   |
| 2    | 12.75          | 2.2                 | 4.5                | 0.2                     | 16                   |
| 3    | 36             | 1.4                 | 10.75              | 0.4                     | 16                   |
| 4    | 20             | 0.8                 | 6.63               | 0.3                     | 16                   |

The typical geometry used in the finite element analysis is shown in Figure 3.1. A quadrant is modeled due to the inherent symmetry of the geometry. The inside surface of the piping run was prescribed a temperature equal to the steam temperature in the pipe. The external surface of the piping run was assumed to be insulated. Various insulation scenarios were studied for the trunnion, each of which involved a portion of the external surface of the trunnion being insulated (the portion adjacent to the piping run) and a portion being uninsulated (the remaining length of the trunnion). The uninsulated region of the trunnion was assigned a natural convection coefficient to simulate heat transfer with the ambient air around the trunnion (nominal air temperature assumed to be 70F). The inside surface of the trunnion was assumed to be insulated, approximating the poor (negligible) heat transfer that would likely occur on that surface because of the lack of any ambient (cooling) air circulating within the trunnion. Some cases were also analyzed in which a cap (flat plate) was added to the end of the trunnion; the external face of this cap was assumed to have a natural convection coefficient similar to that of the uninsulated portion of the trunnion.

For the steady-state heat conduction analysis the only relevant material property is the thermal conductivity of the steel (Grade 91) which was specified as 16Btu/h-ft-F; because the thermal conductivity of Grade 91 steel varies little with temperature then this single value was selected to simplify the analyses without compromising the generality of the results and subsequent conclusions.

The complete matrix of cases analyzed (with details of the assumed insulation thickness and natural convection coefficient) is summarized in Table 3-2. The case number refers to the overall pipe and trunnion geometry documented in Table 3-1 and the corresponding pipe outside diameter is included in the table for reference. The insulation thickness (the length of trunnion buried in insulation) was varied from 0 (no insulation) to 8in (half the trunnion length). It is recognized that zero insulation thickness is not a practical case because some portion of the trunnion is always buried in the insulation associated with the pipe run, but was included to provide an overall trend. Finally, the film coefficient has been varied on these cases between 0.2 and 1.7 Btu/hr-ft<sup>2</sup>-F to simulate stagnant air and an area with some air flow, respectively. The case of stagnant air would be representative of the Lisega type 48 pipe supports where the pipe support itself limits the heat loss from the trunnion. The case of higher air flow would represent a trunnion which is out in the open with little restriction in its immediate vicinity, where no obstructions impact the environment from removing heat from the trunnion.

**Table 3-2**  
**Matrix of steady state thermal cases analyzed**

| Case | Pipe O.D. (in) | Insulation Thickness (in) | Natural Convection Coefficient (Btu/hr-ft <sup>2</sup> -F) |
|------|----------------|---------------------------|--|
| 1    | 24             | 0                         | 0.2  |
|      |                |                           | 1.7  |
|      |                | 4                         | 0.2  |
|      |                |                           | 1.7  |
|      |                | 8                         | 0.2  |
|      |                |                           | 1.7  |
| 2    | 12.75          | 0                         | 0.2  |
|      |                |                           | 1.7  |
|      |                | 4                         | 0.2  |
|      |                |                           | 1.7  |
|      |                | 8                         | 0.2  |
|      |                |                           | 1.7  |
| 3    | 36             | 0                         | 0.2  |
|      |                |                           | 1.7  |
|      |                | 4                         | 0.2  |
|      |                |                           | 1.7  |
|      |                | 8                         | 0.2  |
|      |                |                           | 1.7  |
| 4    | 20             | 0                         | 0.2  |
|      |                |                           | 1.7  |
|      |                | 4                         | 0.2  |
|      |                |                           | 1.7  |
|      |                | 8                         | 0.2  |
|      |                |                           | 1.7  |

In addition, several other analyses were performed to investigate the effect of adding an end cap, as documented in Table 3-3. As with the previous table, the case number refers back to the geometric data provided in Table 3-1. Only Case 1 was considered for the end cap because the intent was simply to explore the relative effect of an end cap.

**Table 3-3**  
**Matrix of end cap steady state thermal cases evaluated**

| Case | Pipe O.D. (in) | Insulation Thickness (in) | Natural Convection Coefficient (Btu/hr-ft <sup>2</sup> -F) | End Cap Thickness (in) | End Cap Width and Height (in) |
|------|----------------|---------------------------|--|------------------------|-------------------------------|
| 1    | 24             | 0                         | 0.2  | 1                      | 10                            |
|      |                |                           |  | N/A                    | N/A                           |
|      |                | 0                         | 1.7  | 1                      | 10                            |
|      |                |                           |  | N/A                    | N/A                           |
|      |                | 4                         | 0.2  | 1                      | 10                            |
|      |                |                           |  | N/A                    | N/A                           |
| 4    | 1.7            | 1                         | 10   |                        |                               |
|      |                | N/A                       | N/A  |                        |                               |

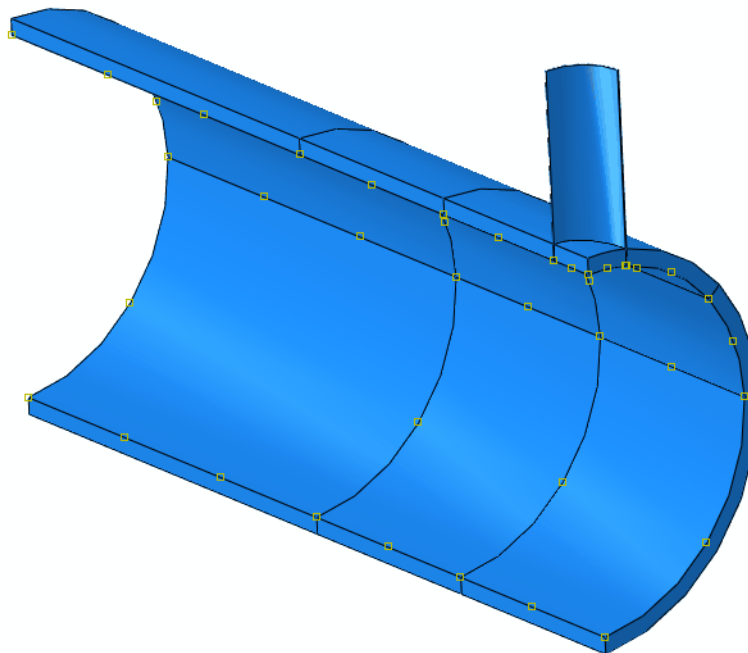


**Figure 3-1**  
**Typical finite element model for steady state thermal evaluation**

### 3.2 Results and Discussion for Steady State Thermal Analyses

The general trends in temperature distribution as a function of some of the key parameters are documented in the following tables and figures. The influence of natural convection coefficient is illustrated in Figures 3-2 and 3-3 which, respectively, show temperature distributions for natural convection coefficients of 1.7Btu/hr-ft<sup>2</sup>-F and 0.2Btu/hr-ft<sup>2</sup>-F. In both of these figures the



trunnion is assumed to be uninsulated. The higher film coefficient results in a much greater heat loss from the trunnion giving a temperature at the end of the trunnion of approximately 175F, whereas the lower film coefficient gives a temperature at the end of the trunnion of approximately 750F.

To more clearly illustrate the temperature reduction at the pipe to trunnion junction (weldment), Figures 3-4 and 3-5 illustrate the temperature difference (fluid temperature minus metal temperature) on the pipe and trunnion for natural convection coefficients of 1.7Btu/hr-ft<sup>2</sup>-F and 0.2Btu/hr-ft<sup>2</sup>-F, respectively. From these figures it can be seen that the temperature at the base of the trunnion where the weld would be located is lower than the temperature of the pipe itself, but only by a relatively modest amount (~10 to 60F).

To document the overall trends from the various analyses, Figure 3-6 shows the variation in temperature difference (between the steam in the pipe run and the base of the trunnion where the weld is located) with insulation thickness for each of the 4 cases (geometries), with the two natural convection film coefficients. The results on Figure 3-6 form two distinct groups based on the magnitude of the film coefficient, with the lower value of film coefficient grouping the results in the lower portion of the plot. Evidently there is only a significantly lower temperature at the pipe to trunnion junction when the trunnion is uninsulated and experiences a higher natural convection film coefficient (representative of good airflow around the trunnion). Obviously the uninsulated trunnion is not a feasible configuration (the trunnion is at least buried in insulation to the thickness of the insulation on the line to which it is attached) hence for practical configurations there is a relatively modest temperature reduction at the pipe to trunnion junction, of the order of 5F to 15F. Such a temperature reduction at the pipe to trunnion junction (weld) would likely only have a modest effect on local creep damage accumulation (typically a 25F temperature reduction would result in approximately a doubling of the creep lifetime at a given stress).

The effect of an end cap on the trunnion is documented in Figure 3-7, which shows the temperature difference (between the steam in the pipe run and the base of the trunnion where the weld is located) as a function of trunnion length. Various plots in the figure show the effect of end cap or no end cap, and the effect of natural convection coefficient. The influence of 4in of insulation is also included. The results in this figure again divide into two groups: one group for a natural film coefficient of 1.7Btu/hr-ft<sup>2</sup>-F and another group for a natural film coefficient of 0.2Btu/hr-ft<sup>2</sup>-F. There is a large variance in temperature difference (steam temperature to weld junction metal temperature) between these two groups. The effect of the end cap (or not) is most evident in the results with the higher natural convection film coefficient and with shorter trunnion lengths. When the trunnion length is short (less than ~8in) and when it has an end cap then the end cap provides additional surface from which natural convection can occur and this results in a lower temperature (by approximately 10F) at the pipe to trunnion weld. As trunnion length is increased this effect diminishes. In reality, most trunnions in that size range will be at least partially insulated and will likely include some clamping/support arrangement that may impede air flow, resulting in a lower film heat transfer coefficient which will negate any benefit associated with a cap on the trunnion.

A further influence on steady state temperatures will be the effect of any clamp or support to which the trunnion is attached. Depending on the arrangement, this may act to impede air flow and limit convective heat transfer, or may act as a heat path for conduction which could

substantially decrease the trunnion temperature (even back at the pipe to trunnion connection). However, in many trunnion arrangements the coupling to the support structure is based on a sliding fit (e.g., trunnion inside a hole in the support frame) and the effectiveness of conduction will be very dependent on largely indeterminate parameters such as contact area and local oxidation. As a result, while it is possible that certain support structures may result in a lower temperature at the pipe to trunnion connection it is not recommended to take credit for that unless this can be proven with certainty through a detailed audit of the actual, as-built, configuration.

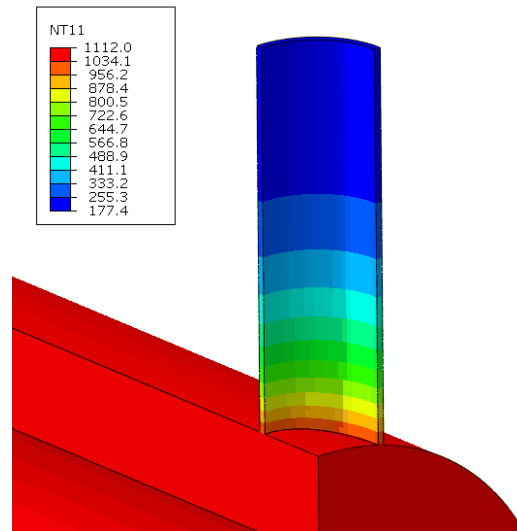


**Figure 3-2**  
Color contour plot showing temperature (F) distribution for Case 1 with 1.7Btu/hr-ft<sup>2</sup>-F natural convection coefficient

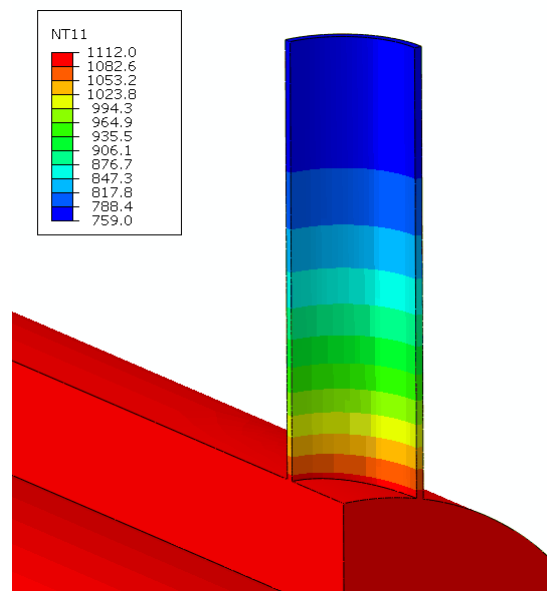


**Figure 3-3**  
Color contour plot showing temperature (F) distribution for Case 1 with 0.2Btu/hr-ft<sup>2</sup>-F natural convection coefficient

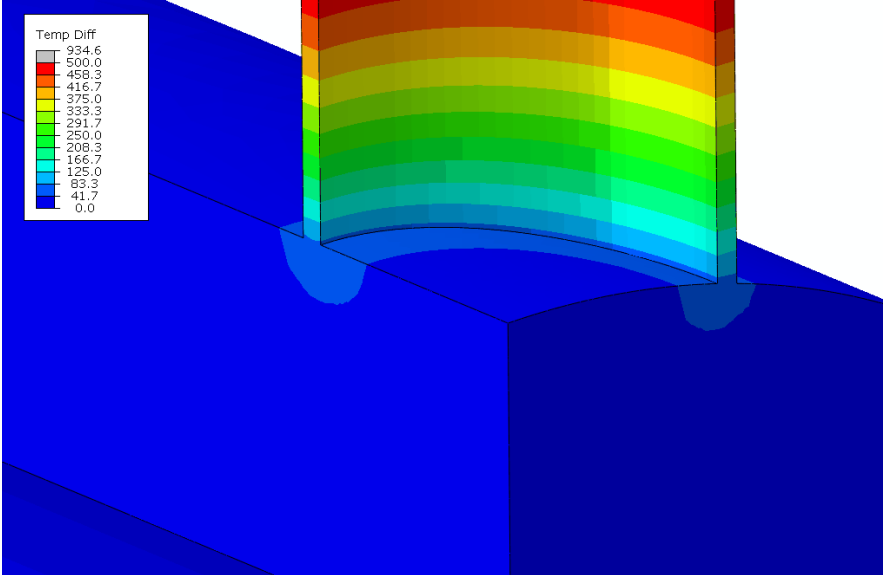


**Figure 3-4**  
Color contour plot showing temperature difference (F) in Case 1 with 1.7Btu/hr-ft<sup>2</sup>-F natural convection coefficient

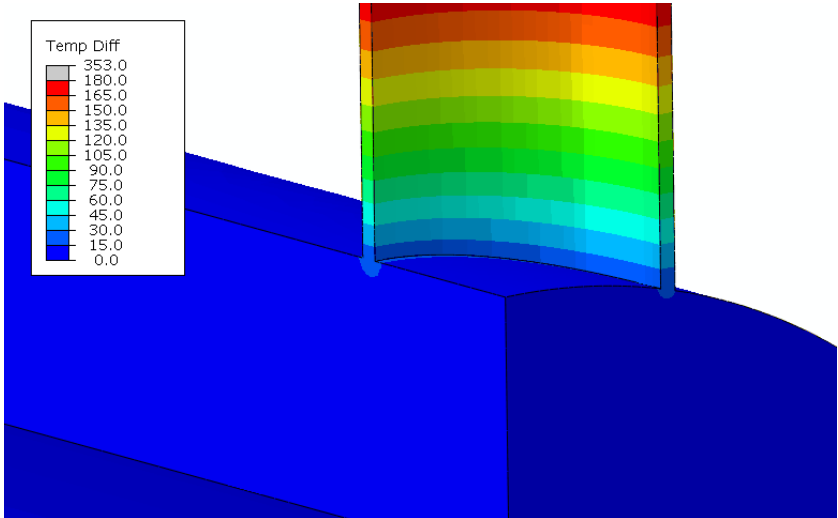


**Figure 3-5**  
Color contour plot showing temperature difference (F) in Case 1 with 0.2Btu/hr-ft<sup>2</sup>-F natural convection coefficient

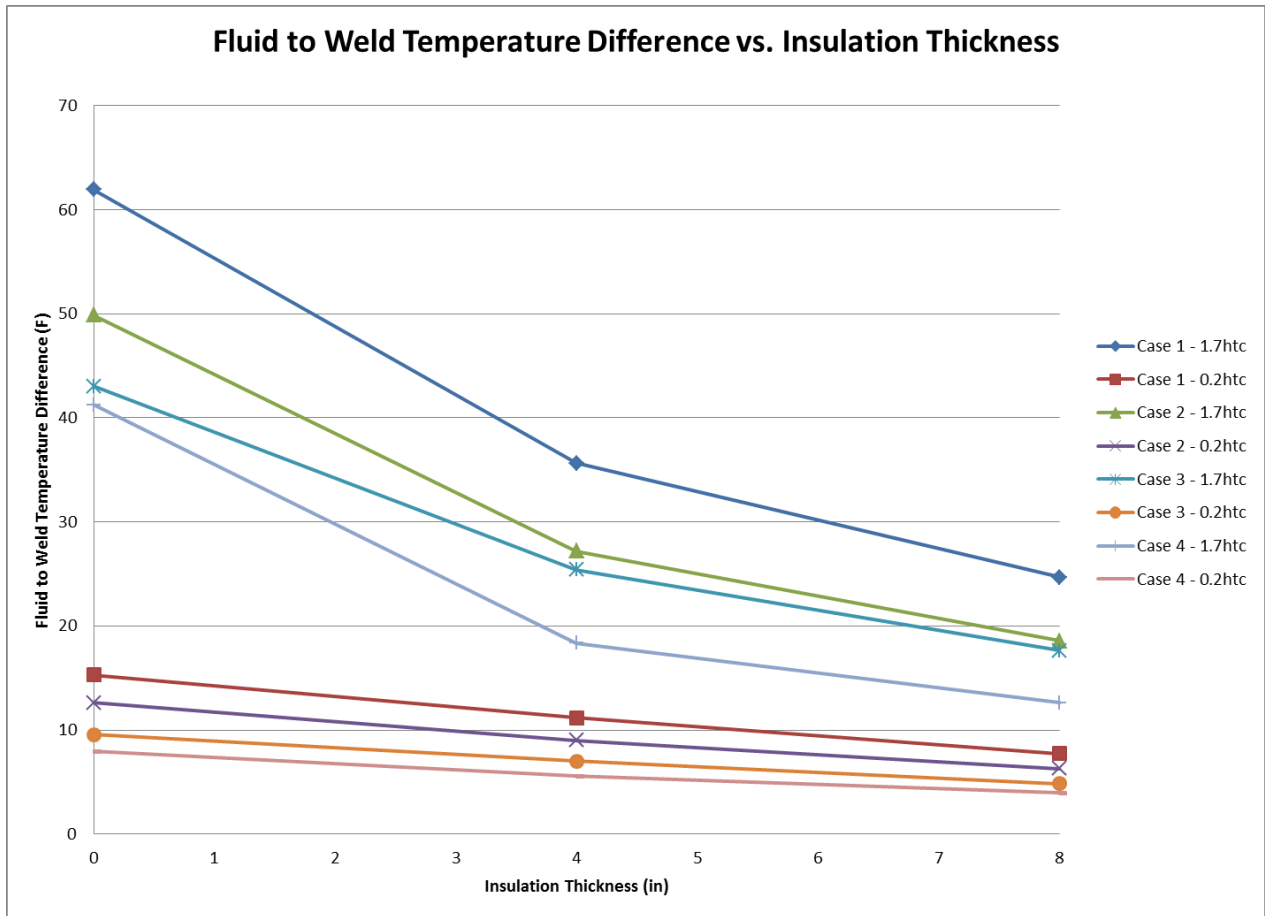


**Figure 3-6**  
Fluid to weld temperature difference (F) as a function of insulation thickness for various heat transfer coefficients and configurations

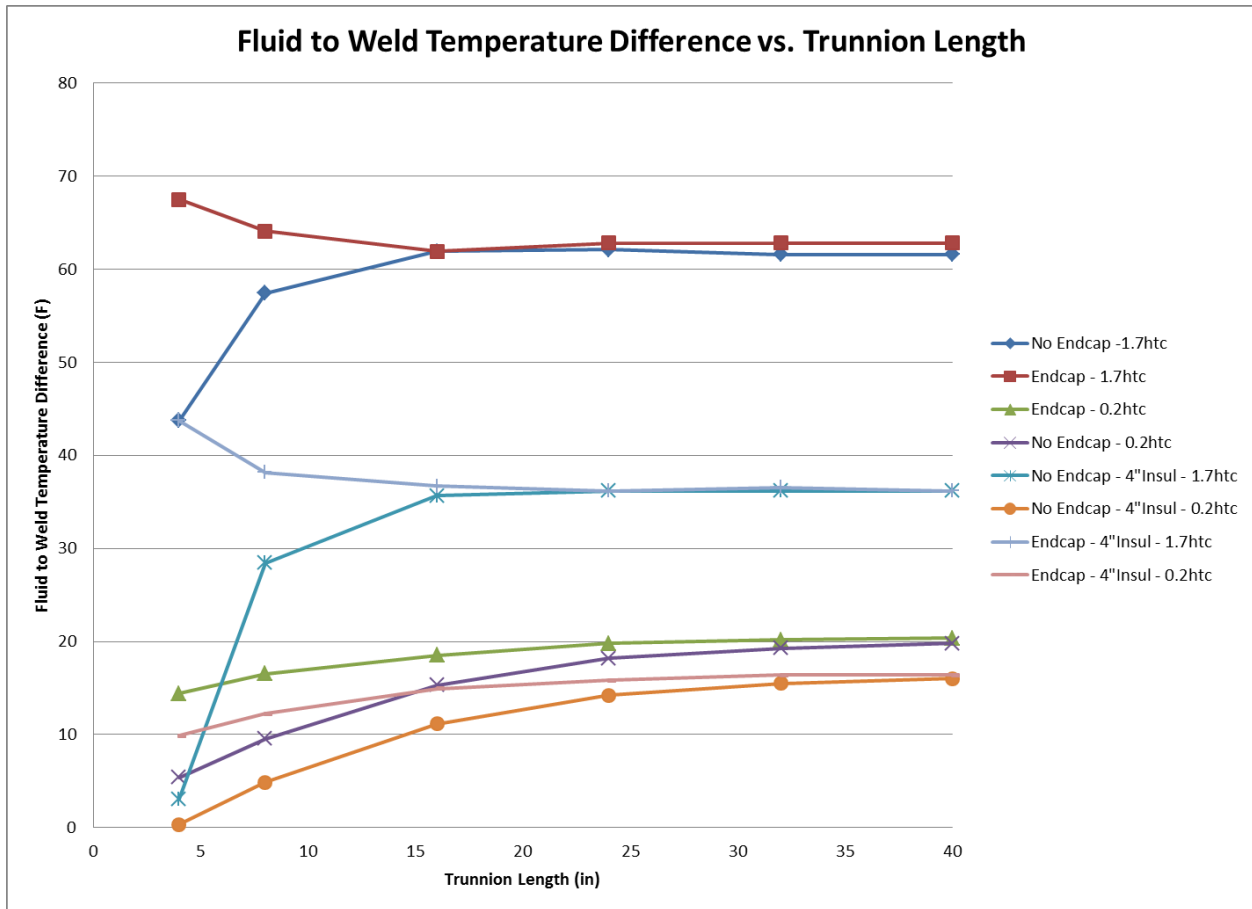


**Figure 3-7**  
Fluid to weld temperature difference (F) as a function of trunnion length for various heat transfer coefficients, illustrating the effect of an end cap for the Case 1 configuration

### 3.3 Conclusions from Steady State Thermal Analyses

The preceding analyses demonstrate that the temperature at the pipe to trunnion weld is controlled by many factors, most dominantly by the amount of insulation on the trunnion, the length of the trunnion, and the natural film coefficient. As it is generally the case on Grade 91 piping system that the insulation thickness is approximately 8in then even for a trunnion protruding out of that insulation there is only a 15F benefit (lowering of temperature) at the pipe to trunnion interface for the case with a relatively high natural convection film heat transfer coefficient, and less than a 5F benefit for the case of a poor (low) natural convection film heat transfer coefficient. Hence it is difficult to justify taking any credit for a lower temperature (and hence potentially a reduction in the rate of any creep damage accumulation) at the pipe to trunnion weld.

Therefore, when assessing which trunnions might be included in an inspection program, it is not recommended to consider so-called “uninsulated” trunnions as being at measurably lower risk of creep damage than fully insulated trunnions. Also, the presence (or lack of) an end cap is not a significant discriminator either. Furthermore although certain support structures for the trunnion may offer a path for heat conduction, the as-built configuration (alignment, tolerances, oxidation) will significantly affect the local temperatures and hence it is not recommended to take any credit (temperature reduction at the trunnion to pipe weld) for such heat conduction paths.

# 4

## STEADY STATE TEMPERATURES

---

The previous section on steady-state temperature distribution determined that, in general, a trunnion cannot be relied upon as an effective heat sink, so the temperature at the base of the trunnion during periods of steady state operation should conservatively be taken as the corresponding steam temperature. This section of the report explores the effect of thermal transients; that is the period of temperature change to, or from, the steady state condition. During these transients the trunnion is heated (during a temperature rise, or cooled during a temperature drop) by conduction through the pipe to trunnion weld. During heating the trunnion will generally be at a lower temperature than the pipe to which it is attached which will create a thermal stress at the pipe to trunnion connection (weld). The magnitude of this thermal stress is important because, if sufficiently large, it could result in accumulation of fatigue damage at the pipe to trunnion weld—particularly for plants that experience a large number of cycles (such as combined cycle plants that are often on a daily cycling regime).

As with the steady state temperature distribution, a series of finite element models has been used to explore the transient temperature distributions and the resulting thermal stresses for a range of key parameters related to the pipe and trunnion configuration. The following subsections explain the analysis model, discuss the results and summarize the key conclusions.

### 4.1 Transient Analysis Model

A matrix of pipe and trunnion dimensions was selected, as documented in Table 4-1, to bound typical configurations for main-steam and hot reheat piping systems of utility and combined cycle plants. The trunnion length was specified at what is regarded as a typical length of longer trunnions (which are likely to have higher thermal stresses) as is often the case when trunnions are connected directly to pipe supports or saddles. Shorter trunnions are used in other configurations (such as with a Lisega type 48 riser clamp), but these will inherently have a lower stress. This effect of trunnion length is addressed in more detail later in this section. The typical configuration for the geometric model is shown in Figure 4-1. Only a quadrant of the geometry is modeled to take advantage of the inherent symmetry. This is possible for the analyses here because they only explore temperatures and the resulting thermal stresses (no mechanical loading on the trunnion).

For the analyses here, the weld between the pipe and trunnion is not explicitly modeled. That is, the trunnion is connected directly to the pipe with no weld reinforcement or other condition. Review of actual trunnion configurations reveals that the pipe to trunnion weld is invariably of full penetration so neglecting any weld reinforcement (fillet) will underestimate the throat area which will, in turn, result in a smaller area for heat conduction (thereby giving a greater temperature differential between the pipe and trunnion and hence a higher thermal stress). For

the stress analysis, neglecting the weld fillet creates a sharp transition, with an associated stress singularity, which causes locally unrealistic stresses in the finite element results but this is dealt with by using stress linearization across the section to remove the contribution from the stress singularity and give a “structural stress” that can be used for life assessments.

**Table 4-1**  
**Key geometric data of transient cases**

| Case | Pipe O.D. (in) | Pipe Thickness (in) | Trunnion O.D. (in) | Trunnion Thickness (in) | Trunnion Length (in) |
|------|----------------|---------------------|--------------------|-------------------------|----------------------|
| 1    | 24             | 4.1                 | 6.63               | 0.3                     | 16                   |
| 2    | 12.75          | 2.2                 | 4.5                | 0.2                     | 16                   |
| 3    | 36             | 1.4                 | 10.75              | 0.4                     | 16                   |
| 4    | 20             | 0.8                 | 6.63               | 0.3                     | 16                   |

The boundary conditions applied to the model assumed, for simplicity, that the entire exterior surface of the pipe and trunnion were perfectly insulated. Appropriate symmetry boundary conditions were specified on the symmetric faces of the quadrant modeled. The end of the piping run away from the trunnion was specified to remain plane. For the parametric analyses here, a simple linear thermal ramp rate (change of steam temperature with time) was applied to the internal surface of the main piping run (specifying the pipe inside temperature avoids the need to define a film heat transfer coefficient and conservatively represents perfect heat transfer from the steam to the pipe). This temperature ramp rate was changed to determine the effect on stresses at the pipe to trunnion weld.

For simplicity, since the objective here is only to understand the relative magnitudes of stresses (not to determine accurate stresses for a particular case which could then be used for a life assessment), the material properties were taken as typical values for Grade 91 steel, with no temperature dependence (the properties are appropriate for a nominal temperature of 600F, which is approximately the average temperature during the analysis). **Error! Reference source not found.**4-2 summarizes these properties.

**Table 4-2**  
**Relevant material data for steady state thermal evaluation**

| Material | Thermal Conductivity (Btu/h-ft-F) | Density (lb <sub>m</sub> /ft <sup>3</sup> ) | Young's Modulus (ksi) | Coefficient of Thermal Expansion (abs/C) | Specific Heat (Btu/lb <sub>m</sub> -F) |
|----------|-----------------------------------|---|-----------------------|--|--|
| Grade 91 | 16                                | 475   | 28500                 | 1.16E-5                                  | 0.13                                   |

In addition to the base cases documented in Table 4-1, a number of other cases were run to provide a greater range of parameters to help identify trends between geometry and stress magnitude with a view to developing an approximate criterion for ranking the likely susceptibility of a particular configuration to thermal transients. These cases are summarized in Table 4-3. Of these, Case 5 represents an actual trunnion design, while Case 6 is a modification of this design to examine the effect of trunnion thickness on the system. Similarly, Cases 7 and 8 are modifications of Case 1 with a larger trunnion wall thickness. Cases 9 and 10 are



modifications of Case 1 with both a larger and a smaller trunnion diameter, respectively. Cases 11 and 12 are modifications of Case 1 with both a longer and shorter trunnion length, respectively. Finally, Cases 13 through 16 are modifications of Case 1 with changes to both the pipe thickness and trunnion thickness to explore the effect of having extremes of each present. It should be recognized that some of these Cases do not represent practical design selections; they are merely to explore the parameters that significantly affect the stress at the pipe to trunnion weld.

**Table 4-3**  
**Additional finite element cases analyzed**

| Case | Pipe O.D. (in) | Pipe Thickness (in) | Trunnion O.D. (in) | Trunnion Thickness (in) | Trunnion Length (in) |
|------|----------------|---------------------|--------------------|-------------------------|----------------------|
| 5    | 20             | 3.4                 | 16                 | 1.6                     | 16                   |
| 6    | 20             | 3.4                 | 16                 | 0.4                     | 16                   |
| 7    | 24             | 4.1                 | 6.63               | 0.9                     | 16                   |
| 8    | 24             | 4.1                 | 6.63               | 0.6                     | 16                   |
| 9    | 24.6           | 4.1                 | 8.63               | 0.3                     | 16                   |
| 10   | 24.6           | 4.1                 | 4                  | 0.3                     | 16                   |
| 11   | 24.6           | 4.1                 | 6.63               | 0.3                     | 24                   |
| 12   | 24.6           | 4.1                 | 6.63               | 0.3                     | 8                    |
| 13   | 24.6           | 4.1                 | 20                 | 4.1                     | 16                   |
| 14   | 24.6           | 0.3                 | 20                 | 4.1                     | 16                   |
| 15   | 24.6           | 4.1                 | 6.63               | 0.1                     | 16                   |
| 16   | 24.6           | 0.3                 | 6.63               | 0.1                     | 16                   |

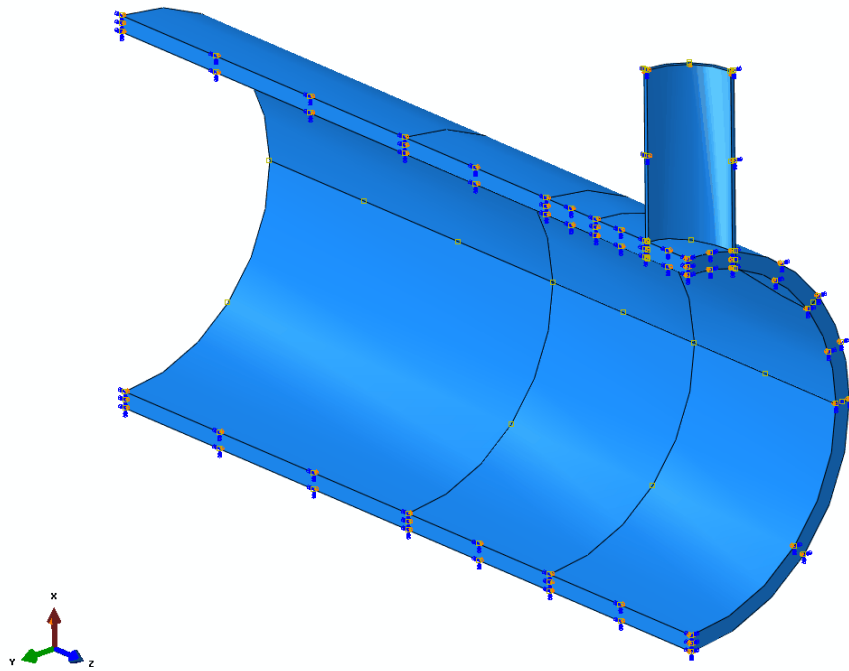


**Figure 4-1**  
Typical finite element model for thermal transient evaluation

## 4.2 Results and Discussion for Transient Analyses

The typical stress distribution produced by the transient is illustrated in Figure 4-2, which shows two views of the stress at the pipe to trunnion junction. The stress distribution is that during the quasi-steady state portion of the transient (that is, the stresses have reached a steady state because the temperature gradient has reached a steady state – even though the temperature continues to increase). The stress distribution is that which occurs on heating of the pipe. The pipe reaches a higher temperature than the trunnion so that the end of the trunnion attached to the pipe is forced to grow to a larger diameter than its temperature would require. This causes a bending stress across the trunnion wall at the interface to the pipe (tension on the outside and compression on the inside of the trunnion wall).

As discussed previously there is an inherent stress singularity so the peak stress magnitude directly from the finite element model cannot be relied on (it is very sensitive to mesh size, which if sufficiently small would give an infinitely large stress). Hence stress magnitudes for each case analyzed are characterized by the linearized through-wall bending stress, as shown in Figure 4-3. This structural bending stress could be used with a fatigue life model to estimate the number of cycles to crack initiation, but here the stress magnitudes for different cases are simply compared to highlight trends as to which parameters create a greater risk of fatigue becoming a problem.

Also for purposes of relative comparison, the through-wall bending stress magnitude at the trunnion are contrasted with the stress magnitude for a penetration in the pipe wall subjected to the same ramp rate (note that a nominal 4-in penetration was used for larger diameter lines and a 2-in diameter penetration was used for smaller diameter lines). This provides a first indication of

the stress magnitude at the trunnion as compared to other features in the piping, such as penetrations. If the stresses are larger at the trunnion than at a typical penetration, then it would imply that the trunnion would be more susceptible to fatigue damage and hence a preferred location for inspection. The typical stress distribution at a penetration in the pipe is shown in Figure 4-4.

The results (stresses) from the preliminary cases (1 through 4) are documented in Table 4-4, which includes the surface bending stress at the base of the trunnion, the stress (biaxial compression on heating) at the inside surface of the pipe and the stress at the edge of a penetration in the piping. In all cases these are just the thermal stresses resulting from the uniform temperature ramp. Any mechanical stresses (such as due to internal pressure) are not included. It is apparent that, in some cases, the bending stress at the trunnion can be significantly larger than the stress at the inside surface of the pipe or at the penetration. Hence understanding the parameters that control the stress at the trunnion is important, and why the expanded set of cases defined in Table 4-3 were developed.

The expanded set of cases were all analyzed (as per the previous cases) with a temperature ramp rate of 55F/min. The pseudo steady-state stress magnitude varies linearly with temperature ramp rate (doubling the ramp rate doubles the stress) so stress magnitudes for other ramp rates can be simply estimated.

The results for the expanded set of cases are summarized in Table 4-5 which has been arranged in descending order by trunnion stress magnitude (through-wall bending stress at the base of the trunnion). This illustrates not only which cases have the highest stress in the trunnion, but highlights the parameters that contribute to higher stresses. There is a general trend in the cases with the thicker pipe and trunnion toward the top of the list. Hence a simple screening parameter was conceived as the product of the pipe thickness and trunnion thickness (the last column of Table 4-5). It can be seen that this provides a reasonable ranking of the cases – the principal remaining inconsistency being the effect of trunnion length (shorter trunnions have a lower stress than longer trunnions).

The screening parameter offers a practical tool to assess which trunnions may be at greater risk of fatigue cracking on a given steam line given that all the trunnions on a given line will experience approximately the same thermal transient.

**Table 4-4**  
**Initial thermal transient finite element results**

| Case | Pipe O.D. (in) | Trunnion Stress (ksi) | Inside Stress (ksi) | Penetration Stress (ksi) | Penetration Size (in) | Temperature Ramp Rate (F/min) |
|------|----------------|-----------------------|---------------------|--------------------------|-----------------------|-------------------------------|
| 1    | 24             | 13.6                  | 14.8                | 16.4                     | 4                     | 54                            |
| 2    | 12.75          | 7.7                   | 4.2                 | 4.7                      | 2                     | 54                            |
| 3    | 36             | 12.3                  | 1.7                 | 2.1                      | 4                     | 54                            |
| 4    | 20             | 6.6                   | 0.5                 | 0.7                      | 2                     | 54                            |

**Table 4-5**  
**All thermal transient finite element results**

| Case | Pipe O.D. (in) | Pipe Thickness (in) | Trunnion O.D. (in) | Trunnion Thickness (in) | Trunnion Length (in) | Trunnion Stress (ksi) | Trunnion Thickness Pipe Thickness (in <sup>2</sup> ) |
|------|----------------|---------------------|--------------------|-------------------------|----------------------|-----------------------|--|
| 13   | 24             | 4.1                 | 20                 | 4.1                     | 16                   | 75.5                  | 17   |
| 5    | 20             | 3.4                 | 16                 | 1.6                     | 16                   | 51.3                  | 5.4  |
| 7    | 24             | 4.1                 | 6.63               | 0.9                     | 16                   | 27.2                  | 3.6  |
| 8    | 24             | 4.1                 | 6.63               | 0.6                     | 16                   | 22                    | 2.3  |
| 6    | 20             | 3.4                 | 16                 | 0.4                     | 16                   | 19.1                  | 1.3  |
| 11   | 24             | 4.1                 | 6.63               | 0.3                     | 24                   | 16.7                  | 1.2  |
| 9    | 24             | 4.1                 | 8.63               | 0.3                     | 16                   | 14.7                  | 1.2  |
| 1    | 24             | 4.1                 | 6.63               | 0.3                     | 16                   | 13.6                  | 1.2  |
| 14   | 24             | 0.3                 | 20                 | 4.1                     | 16                   | 12.8                  | 1  |
| 10   | 24             | 4.1                 | 4                  | 0.3                     | 16                   | 12.3                  | 1.2  |
| 3    | 36             | 1.5                 | 10.75              | 0.4                     | 16                   | 12.3                  | 0.6  |
| 12   | 24             | 4.1                 | 6.63               | 0.3                     | 8                    | 9.5                   | 1.2  |
| 15   | 24             | 4.1                 | 6.63               | 0.1                     | 16                   | 8.3                   | 0.5  |
| 2    | 12.75          | 2.2                 | 4.5                | 0.2                     | 16                   | 7.7                   | 0.5  |
| 4    | 20             | 0.8                 | 6.63               | 0.3                     | 16                   | 6.6                   | 0.2  |
| 16   | 24             | 0.3                 | 6.63               | 0.1                     | 16                   | 2.8                   | 0.1  |

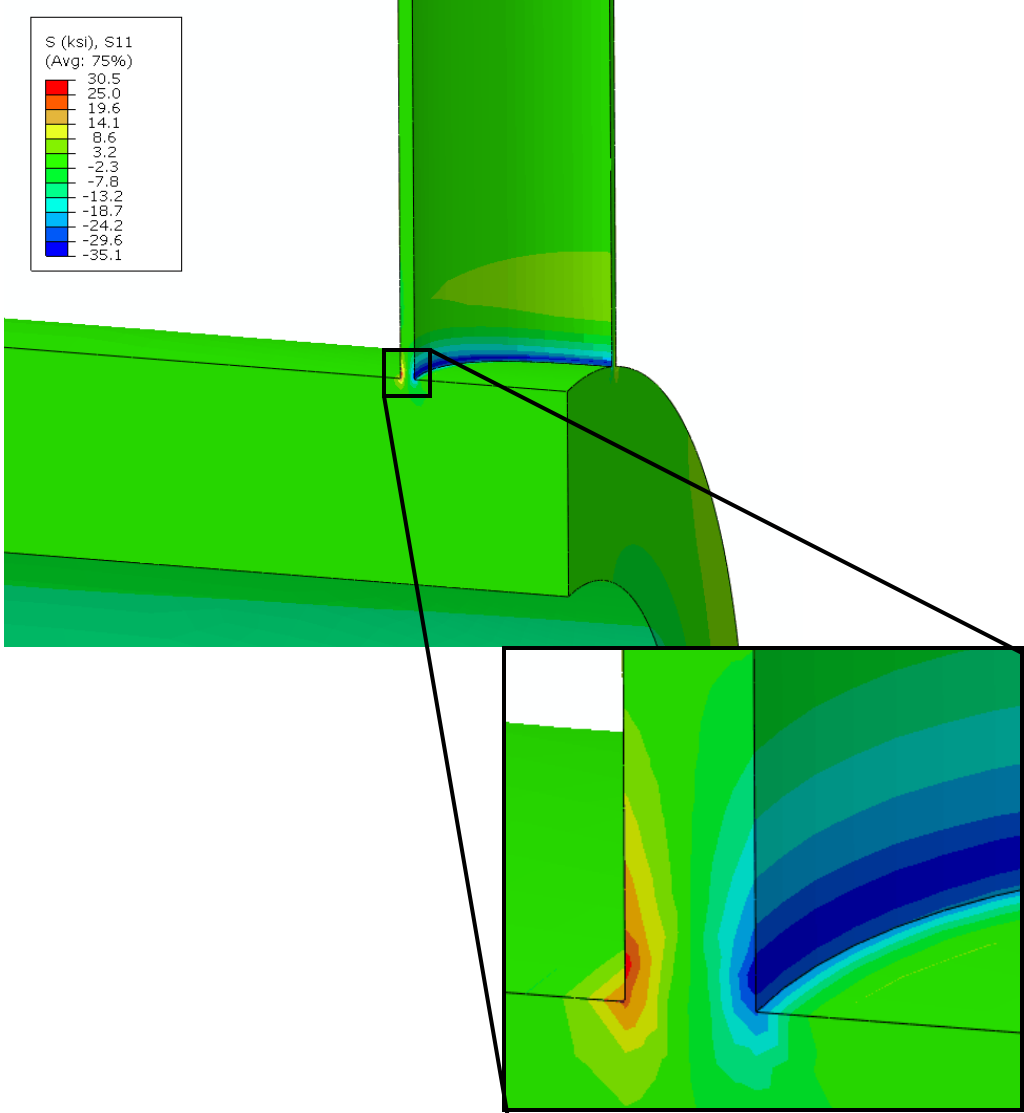


**Figure 4-2**  
Color contour plot of the bending stress (ksi) at the base of the trunnion due to a heating transient in the pipe

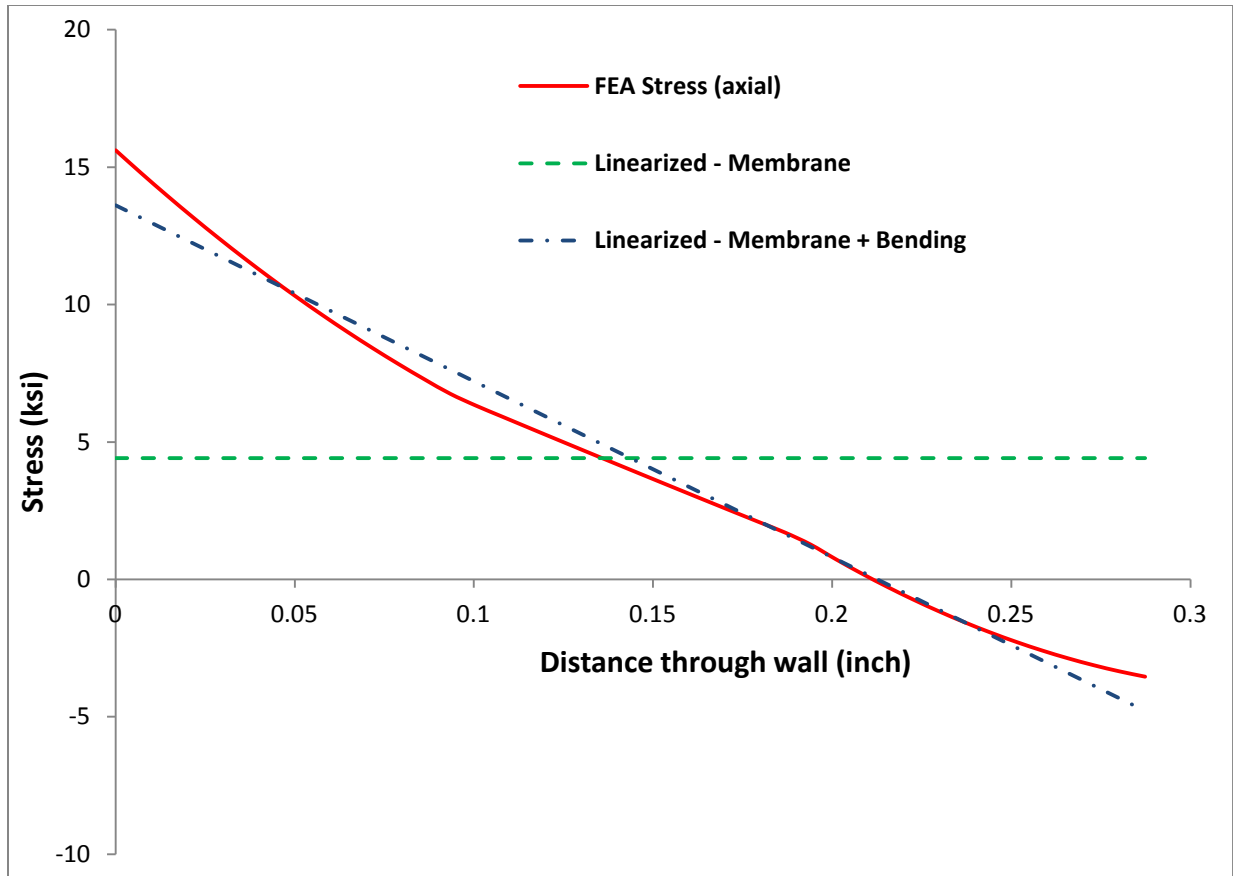


**Figure 4-3**  
Chart showing the through wall bending stress across the trunnion thickness and the linearization of the stress distribution (for Case 1)

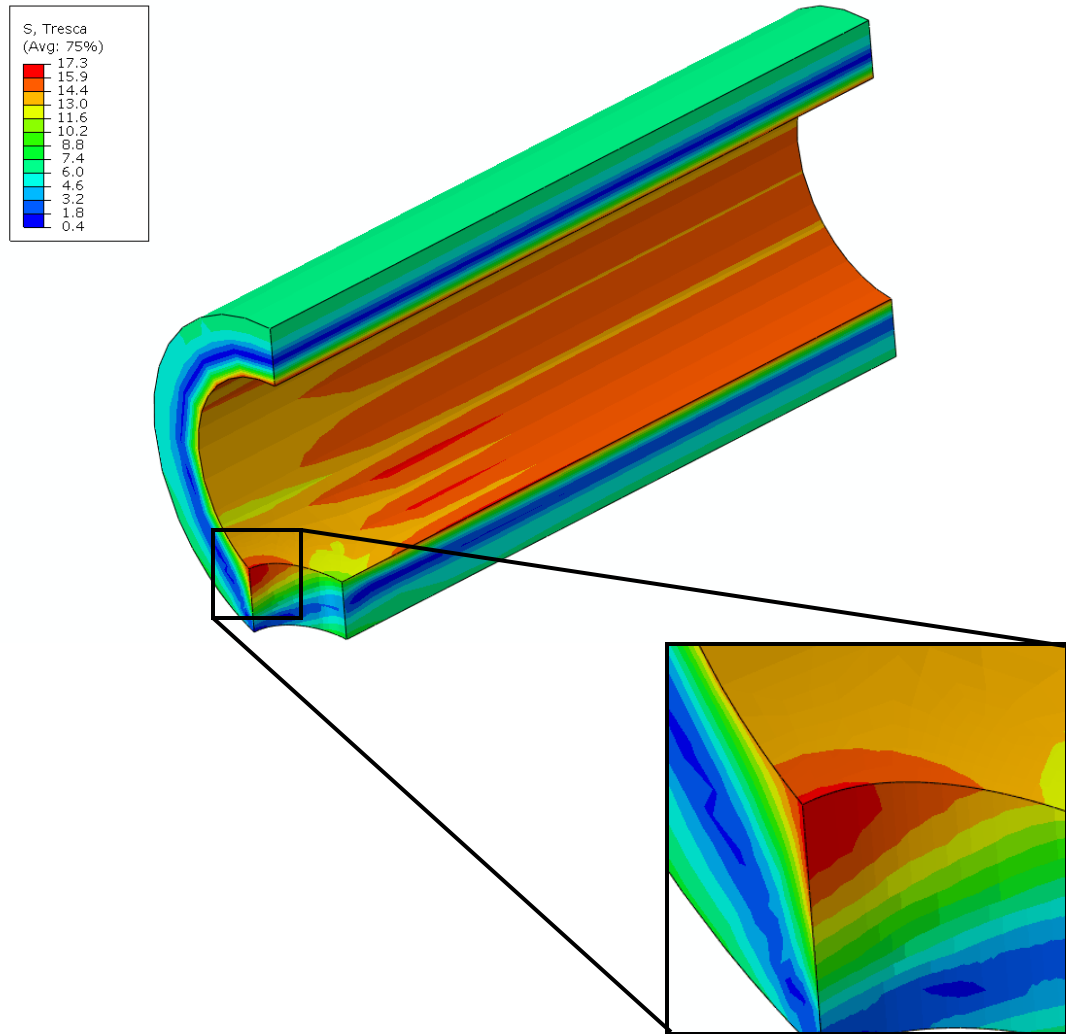


**Figure 4.4**  
Color contour plot showing the Tresca stress distribution (ksi) for a penetration in the pipe (configuration per Case 1) for a heating thermal transient

### 4.3 Conclusions from Transient Analyses

The analyses of the pipe and trunnion subjected to a steam temperature transient inside of the pipe demonstrate that a significant bending stress can occur at the base of the trunnion where it connects to the pipe. If of sufficient magnitude, this stress could cause initiation of a fatigue crack at the toe of the weld on the trunnion side of the connection. Due to the through-wall bending characteristic, which reverses from tension on the outside for heating of the pipe to tension on the inside for cooling of the pipe, then it is possible that crack initiation could occur from either the outside surface of the trunnion or the inside surface. As with many welded connections, which side is more critical will be highly dependent on weld quality. However, if the piping is known to have experienced rapid cooling (e.g., downshocks from condensate) then it would be prudent to perform inspection of the pipe to trunnion weld for both internal and

external cracking (e.g., using an ultrasonic technique). If the piping experiences rapid heating on startup and slow cooling on shutdown then cracking is more likely on the outer surface of the trunnion (at the toe of the weld) and simple penetrant or magnetic particle inspection may be adequate.

Comparison with the magnitude of other thermal stresses (for similar steam temperature ramp rates) indicates that the bending stress at a trunnion can, in some cases, be larger than the thermal stress on the inside surface of the pipe, or at a penetration in the pipe. Hence if the unit is subject to significant cycling with relatively rapid rates of temperature change, such as might occur for a combined cycle plant then it would be prudent to assess any trunnions to determine which may be at higher risk and therefore warrant inspection or a specific analysis.

To establish which trunnions have a greater likelihood of cracking an approximate screening criterion can be used, as was indicated directly from the preceding analysis results. The aim of the screening criterion is not to accurately estimate stresses for a life prediction, but to simply estimate which trunnions are likely to have a higher stress and therefore would be a higher priority for inspection (obviously if the higher priority trunnions do not have evidence of damage then the remaining trunnions are even less likely to have damage). Following the basic theory for transient thermal stress, a simple screening criterion can be defined as:

$$R_T = \frac{\theta T t}{\lambda}$$

Where:  $R_T$  = Risk factor for thermal transients

$\theta$  = Rate of temperature change

$T$  = Pipe thickness

$t$  = Trunnion thickness

$\lambda$  = Thermal diffusivity of material

It should be recognized that this is a simplified risk screening factor, not an accurate stress calculation (the screening factor actually has dimensions of temperature; related to the temperature difference between the pipe and trunnion which drives the stress but, again, this is not a temperature difference predictor either). Hence this parameter should only be used as a relative screening factor to determine which trunnion(s) inspections or further analyses should be conducted on. Should the worst trunnion(s) be found to not limit the future serviceability, it can be concluded that trunnions with a lower screening factor are not a concern.



# 5

## SUMMARY AND RECOMMENDATIONS

---

Trunnions are increasingly used for support of main-steam and hot reheat lines of both supercritical utility and combined cycle plants. Invariably these piping systems are fabricated from creep strength enhanced ferritic steels, such as Grade 91. A challenge with these creep strength enhanced steels is that they usually have significant weld strength reduction factors due to the inherent weakness of the type IV region of the heat affected zone under creep conditions. This has only recently been recognized by boiler design codes (e.g., ASME Section I, 2008 edition) but does not appear to have (yet) influenced trunnion design rules. Indeed, trunnion design rules themselves are not formalized and it has been demonstrated in this report that several design approaches are possible (within the requirements of ASME B31.1 Power Piping, to which most piping systems are designed); although all appear to have conservatism (some excessive). Based on the review of design methods, and from an ad-hoc review of a number of actual trunnion configurations installed on main-steam and hot reheat piping systems, it appears that whatever rules were applied result in configurations that should have a reasonable lifetime in that the stresses are generally within acceptable limits, even for the phenomenon of type IV damage.

Therefore, it does not appear that undue concern needs to be raised about the possibility of trunnion damage/failure, however the ad-hoc sampling of actual trunnions considered in this report does not cover all possible practical configurations. To help identify which trunnions on a piping system (or between multiple systems) might be more vulnerable a number of simplified calculations have been proposed that can be used in a screening/ranking methodology. The higher ranked trunnion configurations can then be subject to inspection (to detect any evidence of damage) and/or more detailed analysis (to better quantify stresses and likely lifetime/failure mode).

Two principal categories of screening/ranking are defined:

1. For sustained load (illustrated here for the simple case of a single load on the trunnion in either in-plane or out-of-plane direction resulting in a bending moment,  $M$ , at the pipe to trunnion connection) the stresses in the trunnion and pipe can be estimated (for ranking purposes) from:

Estimate the bending stress at the base of the trunnion (connection to pipe)

$$\sigma_{B, trunnion} = \frac{4Mr}{\pi\{r^4 - (r-2t)^4\}}$$

Estimate the induced bending stress in the pipe

$$\sigma_{B, pipe} = \frac{1.17M\sqrt{R}}{\pi r^2 T^{1.5}}$$

Estimate the total stress in the pipe (bending plus other stresses)

a. In-plane:  $\sigma_{pipe,IP} = \sigma_{axial} + \sigma_{B,pipe}$

b. Out-of-plane:  $\sigma_{pipe,OP} = \sigma_{hoop} + \sigma_{B,pipe}$

2. For transient thermal events (heating up or cooling down of the piping) the following parameter can be used for ranking purposes:

$$R_T = \frac{\theta T t}{\lambda}.$$

This parameter does not consider the length of the trunnion, for trunnions having a similar value of screening parameter then the trunnion with greater length to diameter ratio should be ranked as higher priority for inspection and/or analysis. Furthermore, this parameter does not consider the insulation around the trunnion. If the trunnion has little insulation, or if it has an obvious heat conduction path to surrounding structure, then more detailed analysis is recommended.

In addition to the above criteria, some other features related to trunnion configuration are also noted that can increase susceptibility to damage and failure.

- The trunnion and pipe material (and weld filler metal) should be matching. If not then more detailed evaluation is recommended.
- Trunnions with a diameter that is a large fraction of the diameter of the pipe run (e.g., >0.7) may be susceptible to localized type IV creep damage at the saddle of the pipe to trunnion weld (pipe side) even if the load on the trunnion is modest. More detailed analysis is recommended to evaluate the susceptibility of particular trunnions.
- The weld between the pipe and trunnion should be a full penetration weld.
- If reinforcing pads are used around the trunnion then more detailed evaluation should be performed. In general, it is recommended not to use a reinforcing pad in conjunction with a trunnion (indeed, use of reinforcing pads is generally not recommended for any nozzle type connection on superheater or reheater systems, particularly where they are likely to experience significant cyclic operation – e.g., combined cycle plants).
- The trunnion should be insulated to minimize temperature differentials between the pipe and trunnion. Trunnions with little, or no, insulation should be subject to more detailed evaluation, particularly if subject to significant thermal cycling.

With these criteria and accompanying guidelines, the trunnions on any given piping system (or across piping systems) can be ranked in susceptibility to damage from static loads or thermal transients. This provides a helpful basis for selected which trunnions should be subject to inspection (and based on the location of stress–in or out of plane–or the type of loading–static or transient thermal–then the location and type of damage can be used to guide inspection techniques) and/or to more detailed analysis (to provide more accurate stress magnitudes to quantify the likely time to crack initiation and thereby specify an appropriate inspection interval).

# 6

## REFERENCES

---

1. ASME “Power Piping,” B31.1, ASME, New York, NY, 2008.
2. Lisega, Inc. *Standard Supports 2010*. Newport, TN: Lisega, 2010.
3. “Design of Pipe Attachments”, Design Manual – Piping Mechanical, Subject 3810, The M.W. Kellogg Company, 1988.
4. Wichman K.R., Hooper, A.G., Mershon, J.L. “Local Stresses In Spherical and Cylindrical Shells Due to External Loadings” Welding Research Council, Bulletin 107, 1988.
5. Bhattacharya, A. “A Comparison of Simple Analytical Methods for Evaluating Local Stresses at Pipe Support Attachments with Finite Element Analysis Results,” NAFEMS UK Conference, Lincolnshire, UK, 2012.
6. ASME Code Case N-391-2 “Procedure for Evaluation of the Design of Hollow Circular Cross-Section Welded Attachments on Class 1 Piping,” Section III, Division 1, ASME, New York, NY, 1995.
7. ASME Code Case N-392-3 “Procedure for Evaluation of the Design of Hollow Circular Cross-Section Welded Attachments on Classes 2 and 3 Piping,” Section III, Division 1. New York, NY 1994.
8. EN 13480-3 “Metallic Industrial Piping. Part 3: Design and Calculation,” European Committee for Standardization, Brussels, Belgium, 2002.
9. *Stress Indices for Straight Pipe with Trunnion Attachments*, EPRI, Palo Alto, CA: 1998. TR-110162.
10. ASME. Section II Part D. “Material Properties,” New York, NY. 2010.
11. ASME. Section III Division I-Appendices. “Rules for Construction of Nuclear Facility Components,” New York, NY. 2013.





### **Export Control Restrictions**

Access to and use of EPRI Intellectual Property is granted with the specific understanding and requirement that responsibility for ensuring full compliance with all applicable U.S. and foreign export laws and regulations is being undertaken by you and your company. This includes an obligation to ensure that any individual receiving access hereunder who is not a U.S. citizen or permanent U.S. resident is permitted access under applicable U.S. and foreign export laws and regulations. In the event you are uncertain whether you or your company may lawfully obtain access to this EPRI Intellectual Property, you acknowledge that it is your obligation to consult with your company's legal counsel to determine whether this access is lawful. Although EPRI may make available on a case-by-case basis an informal assessment of the applicable U.S. export classification for specific EPRI Intellectual Property, you and your company acknowledge that this assessment is solely for informational purposes and not for reliance purposes. You and your company acknowledge that it is still the obligation of you and your company to make your own assessment of the applicable U.S. export classification and ensure compliance accordingly. You and your company understand and acknowledge your obligations to make a prompt report to EPRI and the appropriate authorities regarding any access to or use of EPRI Intellectual Property hereunder that may be in violation of applicable U.S. or foreign export laws or regulations.

**The Electric Power Research Institute, Inc.** (EPRI, [www.epri.com](http://www.epri.com)) conducts research and development relating to the generation, delivery and use of electricity for the benefit of the public. An independent, nonprofit organization, EPRI brings together its scientists and engineers as well as experts from academia and industry to help address challenges in electricity, including reliability, efficiency, affordability, health, safety and the environment. EPRI also provides technology, policy and economic analyses to drive long-range research and development planning, and supports research in emerging technologies. EPRI's members represent approximately 90 percent of the electricity generated and delivered in the United States, and international participation extends to more than 30 countries. EPRI's principal offices and laboratories are located in Palo Alto, Calif.; Charlotte, N.C.; Knoxville, Tenn.; and Lenox, Mass.

Together...Shaping the Future of Electricity

### **Program:**

Boiler Life and Availability Improvement Program

© 2013 Electric Power Research Institute (EPRI), Inc. All rights reserved. Electric Power Research Institute, EPRI, and TOGETHER...SHAPING THE FUTURE OF ELECTRICITY are registered service marks of the Electric Power Research Institute, Inc.

3002001179